

# Rare Decays and CP Violation in the $B_s$ System

Guennadi Borissov <sup>a</sup>, Robert Fleischer <sup>b,c</sup> and Marie-Hélène Schune <sup>d</sup>

<sup>a</sup>*Department of Physics, Lancaster University, Lancaster LA1 4YB, England, UK*

<sup>b</sup>*Nikhef, Science Park 105, NL-1098 XG Amsterdam, Netherlands*

<sup>c</sup>*Department of Physics and Astronomy, Vrije Universiteit Amsterdam,  
NL-1081 HV Amsterdam, Netherlands*

<sup>d</sup>*LAL, Université Paris-Sud, CNRS/IN2P3, Orsay, France*

## Abstract

CP violating phenomena and rare decays of  $B_s^0$  mesons offer interesting probes to test the quark-flavor sector of the Standard Model. In view of plenty of data reported in particular from the Large Hadron Collider, this topic has received a lot of attention in 2012. We give an overview of the the most recent experimental results, new theoretical developments, and discuss the prospects for the future exploration of the  $B_s^0$ -meson system.

Invited contribution to

*Annual Review of Nuclear and Particle Science*, Vol. **63** (2013)



# 1 Introduction

## 1.1 Setting the Stage

Weak decays of  $B$  mesons offer various strategies for the exploration of the quark-flavor sector of the Standard Model (SM) of particle physics. In the previous decade, decays of  $B_d^0$  and  $B^+$  mesons have been the focus of the  $e^+e^-$   $B$  factories at SLAC and KEK with the BaBar and Belle detectors, respectively. Pioneering first results on the  $B_s^0$ -meson system were first obtained by the ALEPH [1], DELPHI [2] and OPAL [3] experiments at LEP. Few years later the CDF [4–6] and DØ [7, 8] experiments at Fermilab have greatly improved the knowledge of the  $B_s^0$ -meson system. In this decade, the exploration of  $B_s^0$  decays is one of the key topics of the  $B$ -physics program of the Large Hadron Collider (LHC) at CERN, with its dedicated  $B$ -decay experiment LHCb [9].

The valence quark content of a  $B_s^0$  meson is given by a strange quark  $s$  and an anti-bottom quark  $\bar{b}$ . The  $B_s^0$ -meson system exhibits a fascinating quantum-mechanical phenomenon,  $B_s^0$ – $\bar{B}_s^0$  mixing, and provides an interesting laboratory to explore CP violation. Key features of the  $B_s$ -meson system are the large mass difference  $\Delta M_s$  and the expectation of a sizable width difference  $\Delta\Gamma_s$  between the  $B_s$  mass eigenstates, and smallish CP violation in the  $B_s^0 \rightarrow J/\psi\phi$  decay in the SM.

In the SM, all the flavour and CP violation is governed by the Cabibbo–Kobayashi–Maskawa (CKM) quark-mixing matrix [10, 11], connecting the electroweak eigenstates of the down, strange and bottom quarks with their mass eigenstates through a unitary transformation. In extensions of the SM, typically new sources of flavor and CP violation are present, with experimental data putting severe constraints on them. A recent overview of this topic in view of the recent LHC data was given in [12].

The study of the CP asymmetry in mixing offers one of the promising possibilities to search for the new sources of CP violation because of a very small SM expectation. The results of this study using the semileptonic  $B_s^0$  decays obtained at the Tevatron [13–15] show an indication of the deviation from the SM prediction, although the recent measurement by the LHCb experiment [16] is consistent with the SM expectation.

The current results about CP violation in  $B_s^0 \rightarrow J/\psi\phi$  [17–20] and  $B_s^0 \rightarrow J/\psi f_0(980)$  [21, 22] are consistent with the SM corresponding to tiny CP violation. From the theoretical point of view, these measurements are affected by uncertainties from doubly Cabibbo-suppressed penguin contributions [23]– [30]. Since these effects are of non-perturbative nature, they cannot be calculated in a reliable way within QCD. However, the corresponding hadronic parameters can be constrained and determined with the help of control channels.

The study of CP violation in  $B_s^0$  decays is also important for the determination of the angle  $\gamma$  of the unitarity triangle of the CKM matrix. On the one hand, this angle can be determined by means of the pure tree decays  $B_s^0 \rightarrow D_s^\pm K^\mp$ . On the other hand, it can also be extracted from the  $B_s^0 \rightarrow K^+K^-$  decay and its partner channel  $B_d^0 \rightarrow \pi^+\pi^-$ , involving loop contributions.

Complementing these studies of CP violation, the rare decay  $B_s^0 \rightarrow \mu^+\mu^-$  plays an outstanding role for the testing of the SM, where this transition emerges only from loop processes. The theoretical prediction of the branching ratio of this channel involves only

a single non-perturbative, hadronic parameter and is very clean, with an uncertainty limited by lattice QCD. The search for this decay started at the Tevatron [31, 32] and continued at LHC [33–35]. In November 2012, the LHCb collaboration has eventually reported the first evidence of this channel at the  $3.5\sigma$  level, with a branching ratio in agreement with the SM picture although the experimental errors are still large [35].

A further highlight of the experimental  $B_s$  results reported in 2012 is a sizable  $\Delta\Gamma_s$ , which has been established by the CDF, DØ LHCb and ATLAS collaborations [17–20, 36–39]. This quantity leads to subtleties in the conversion of experimental data into branching ratios of  $B_s^0$  decays [40], but offers also new observables that can be exploited in the search for New Physics (NP) with the  $B_s^0 \rightarrow \mu^+\mu^-$  channel [41].

In this review, we shall give an overview of these topics. As a large part will deal with experimental data, let give a brief description of the main detectors in the next subsection.

## 1.2 Experimental Detectors for $B_s^0$ Physics

### 1.2.1 Detectors at Tevatron

The CDF and DØ experiments are general purpose collider detectors designed to maximally exploit the possibilities provided by the  $p\bar{p}$  collisions at  $\sqrt{s} = 1.96$  TeV and operate at the instantaneous luminosity up to  $5 \times 10^{32} \text{ cm}^{-2} \text{ s}^{-1}$ . Although the main emphasis in their design is made on the detection of events with the highest possible invariant mass, they also contain the elements necessary to endeavour the  $B$ -physics research.

Both of them have the tracking system [4, 7] consisting of the solenoidal magnet, the silicon microstrip detectors and the central tracker. The instrumented volume of the CDF tracking system extends up to the radius of 137 cm, while the outer radius of the DØ tracking system is 53 cm.

The muon identification system [5, 8] covers the pseudorapidity range up to  $|\eta| < 1$  in CDF and up to  $|\eta| < 2$  in the DØ detector. The muon system of the DØ experiment also includes the toroidal magnets. They allow an independent measurement of the muon momentum. This property helps to improve the quality of the identified muons.

An important part of the CDF detector essential for the  $B$ -physics studies is its special trigger [6] to select events with displaced tracks. It is the basis for many CDF measurements with fully hadronic  $B$  decays. Its another trigger configurations select the events with one or two muons. The trigger system of the DØ detector does not provide a possibility to collect events with displaced tracks, although its muon and di-muon triggers are very efficient and robust. Therefore the focus of the  $B$ -physics measurements in DØ experiment is shifted towards the semileptonic  $B$  decays and decays with  $J/\psi \rightarrow \mu^+\mu^-$  in the final state.

The polarities of the toroidal and solenoidal magnetic fields of the DØ detector are regularly reversed. This reversal helps to significantly reduce the systematic uncertainties of the measurements sensitive to the differences in the reconstruction efficiency between the positive and negative particles, like the measurements of the  $CP$  violating charge asymmetries.

Thus, both the CDF and DØ experiments have sufficient and powerful tools to fulfill

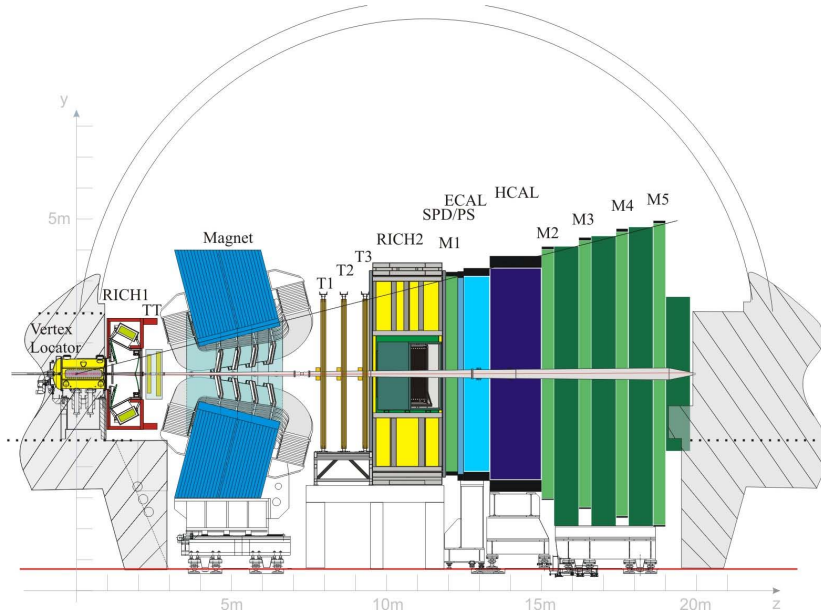


Figure 1: Vertical view of the LHCb detector (from Ref. [9]).

their  $B$ -physics research program. They also contain several special features which make them different and complementary. The CDF detector has a larger tracking volume. Therefore its charged particle momentum resolution is superior to that of the  $D\phi$  detector. It also has the possibility to select the hadronic  $B$  decays. The  $D\phi$  detector includes a sophisticated muon identification system with local measurement of the muon momentum. The reversal of the magnet polarities allows it to perform several measurements of the charge asymmetry in the semileptonic  $B$  decays which are at the world best level.

### 1.2.2 The LHCb detector

The LHCb detector [9], shown in Fig. 1, is a single-arm forward spectrometer covering the pseudorapidity range  $2 < \eta < 5$ , designed for the study of particles containing  $b$ -quark or  $c$ -quark. The detector includes a high precision tracking system consisting of a silicon-strip vertex detector surrounding the  $pp$  interaction region, a large-area silicon-strip detector located upstream of a dipole magnet with a bending power of about 4 Tm, and three stations of silicon-strip detectors and straw drift tubes placed downstream. The combined tracking system has a momentum resolution  $\Delta p/p$  that varies from 0.4% at 5 GeV/ $c$  to 0.6% at 100 GeV/ $c$  and an impact parameter resolution of  $20\mu\text{m}$  for tracks with high transverse momentum. The dipole magnet can be operated in either polarity and this feature is used to reduce systematic effects due to detector asymmetries. Charged hadrons are identified using two ring-imaging Cherenkov detectors. Photon, electron and hadron candidates are identified by a calorimeter system consisting of scintillating-pad and preshower detectors, an electromagnetic calorimeter and a hadronic calorimeter. Muons are identified by a system composed of alternating layers of iron and multiwire proportional chambers.

A two-stage trigger is employed [42]. First a hardware-based decision is taken at a frequency up to 40 MHz. It accepts high transverse energy clusters in either the electromagnetic calorimeter or hadron calorimeter, or a muon of high  $p_T$ . A second trigger level, implemented in software, receives 1 MHz of events and retains  $\sim 0.3\%$  of them. The software trigger requires a two-, three- or four-track secondary vertex with a high sum of the transverse momentum,  $p_T$  of the tracks and a significant displacement from the primary  $pp$  interaction vertices (PVs). At least one track should have  $p_T > 1.7 \text{ GeV}/c$  and impact parameter (IP)  $\chi^2$  with respect to the primary interaction greater than 16. The IP  $\chi^2$  is defined as the difference between the  $\chi^2$  of the PV reconstructed with and without the considered track. A multivariate algorithm is used for the identification of secondary vertices consistent with the decay of a  $b$ -hadron.

### 1.2.3 The Atlas and CMS detectors

The Atlas [43] and CMS [44] detectors are multi-purpose central detectors optimized for searches of heavy objects. At high luminosity, their potential for flavour physics is limited by their triggering capabilities and focus mainly on  $b$  and charmonium decays involving dimuons. Their impact on  $B_s^0$  physics is currently mainly related to the search for the very rare  $B_s^0 \rightarrow \mu^+ \mu^-$  decay and to the study of  $B_s^0 \rightarrow J/\psi \phi$ .

## 1.3 Production of $B_s^0$ Mesons

At the LHC, the  $b\bar{b}$  production cross-section is large: it is expected to be of the order of  $500 \mu\text{b}$  at 14 TeV [45]. The LHC is currently running at 7 or 8 TeV and the cross-section has been measured to be of the order of  $290 \mu\text{b}$  [46] for a center of mass energy of 7 TeV. The detector has taken data at an instantaneous luminosity of about  $3.5$  to  $4 \times 10^{32} \text{ cm}^{-2}\text{s}^{-1}$ , and with a number of  $pp$  interactions per crossing of  $\sim 1.4$ . During the 2012 data taking, the center of mass energy has been increased to  $\sqrt{s} = 8 \text{ TeV}$  which corresponds to an increase of about 15 % in the number of  $b\bar{b}$  events. The recorded data amounts to more than  $3 \text{ fb}^{-1}$ , the world largest  $b$ -hadron sample.

The knowledge of the production rate of  $B_s^0$  mesons is required to determine any  $B_s^0$  branching fraction. To be specific, the measurement of branching ratios of  $B_s^0 \rightarrow f$  decays at hadron colliders relies on certain normalization channels  $B_q \rightarrow X$ , where the  $B_u^+ \rightarrow J/\psi K^+$ ,  $B_d^0 \rightarrow K^+ \pi^-$  and/or  $B_d^0 \rightarrow J/\psi K^{*0}$  modes play key roles. The  $B_s^0$  decay branching ratio can then be extracted with the help of the relation

$$\text{BR}(B_s^0 \rightarrow f) = \text{BR}(B_q \rightarrow X) \frac{f_q \epsilon_X N_{\mu\mu}}{f_s \epsilon_{\mu\mu} N_X}, \quad (1)$$

where the  $\epsilon$  and  $N$  factors denote the total detector efficiencies and the observed number of events, respectively. In practical terms, the ratio of the ‘‘fragmentation functions’’  $f_q$  represents usually the major source of the systematic uncertainty, in particular for the measurement of the branching ratio of the rare  $B_s^0 \rightarrow \mu^+ \mu^-$  decay [47]. The  $f_q$  describe the probability that a  $b$  quark will fragment in a  $\bar{B}_q$  meson ( $q \in \{u, d, s\}$ ), and depend on the hadronic environment of the collider.

A new method for determining  $f_s/f_d$  using nonleptonic  $\bar{B}_s^0 \rightarrow D_s^+ \pi^-$ ,  $B_d^0 \rightarrow D^+ K^-$ ,  $B_d^0 \rightarrow D^+ \pi^-$  decays [47, 48] was implemented at LHCb [49], with a result in good

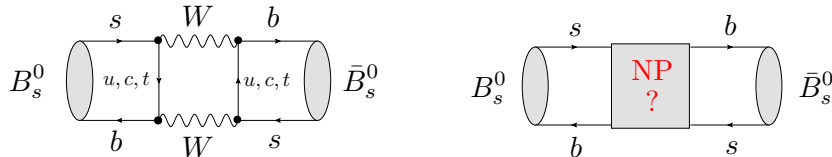


Figure 2: Illustration of  $B_s^0 - \bar{B}_s^0$  mixing in the SM (left panel) and in the presence of NP contributions (right panel).

agreement with measurement using semileptonic decays [50]. The  $SU(3)$ -breaking form-factor ratio entering this method has recently been calculated with lattice QCD [51]. An updated experimental result obtained with the nonleptonic decays and the data recorded in 2011 by the LHCb experiment [52], combined the measurement using semileptonic decays, leads to

$$\frac{f_s}{f_d} = 0.256 \pm 0.020, \quad (2)$$

where the various sources of correlated systematics uncertainties, notably the  $D$  branching fractions and  $B$  lifetimes, are taken into account.

## 1.4 Outline of the Review

The remainder of this review is organized as follows: in Section 2, we discuss  $B_s^0 - \bar{B}_s^0$  mixing and the current status of the measurements of the corresponding mixing parameters. In view of the large value of  $\Delta\Gamma_s$ , we have a closer look at subtleties in the extraction of  $B_s^0$  decay branching ratios and point out the usefulness of effective decay lifetimes. In Section 3, we turn to CP violation in the  $B_s^0$  system, which is a central part of this review. After discussing first CP violation in  $B_s^0 - \bar{B}_s^0$  oscillations that is probed through the semileptonic charge asymmetry, we review the extraction of the mixing phase  $\phi_s$  from the  $B_s^0 \rightarrow J/\psi\phi$  and  $B_s^0 \rightarrow J/\psi f_0(980)$  decays and the associated theoretical uncertainties through penguin topologies. In addition to these benchmark channels, we shall also address CP-violating phenomena in a variety of other  $B_s^0$  decays. In Section 4, we discuss rare  $B_s^0$  decays, with a focus on the most prominent  $B_s^0 \rightarrow \mu^+\mu^-$  channel, and brief discussions of  $B_s^0 \rightarrow \phi\gamma$  and  $B_s^0 \rightarrow \phi\mu^+\mu^-$ . Finally, we summarize in Section 5 the main conclusions and give an outlook of  $B_s^0$  physics.

# 2 Time Evolution of the $B_s^0$ System

## 2.1 General Features

The neutral  $B_s$  mesons show the quantum-mechanical phenomenon of  $B_s^0 - \bar{B}_s^0$  mixing, which is caused in the SM by box-diagram topologies, as illustrated in the left panel of Fig. 2. Consequently, an initially, i.e. at time  $t = 0$ , produced  $B_s^0$ -meson state evolves into a time-dependent linear combination of  $B_s^0$  and  $\bar{B}_s^0$  states:

$$|B_s(t)\rangle = a(t)|B_s^0\rangle + b(t)|\bar{B}_s^0\rangle. \quad (3)$$

The time-dependent functions  $a(t)$  and  $b(t)$  can be calculated in a straightforward way by solving an appropriate Schrödinger equation, where “heavy” and “light” mass eigenstates are introduced, which are characterized by the differences

$$\Delta M_s \equiv M_H^{(s)} - M_L^{(s)}, \quad \Delta\Gamma_s \equiv \Gamma_L^{(s)} - \Gamma_H^{(s)} \quad (4)$$

of their masses and decay widths. These quantities enter the analytic expressions for the time-dependent decay rates  $\Gamma(B_s^0(t) \rightarrow f)$  and  $\Gamma(\bar{B}_s^0(t) \rightarrow f)$ , which correspond to decays of initially present  $B_s^0$  and  $\bar{B}_s^0$  mesons, respectively. Moreover,  $B_s^0$ – $\bar{B}_s^0$  mixing involves also a CP-violating phase, which takes the general form

$$\phi_s = \phi_s^{\text{SM}} + \phi_s^{\text{NP}}. \quad (5)$$

Here the former piece is the SM contribution

$$\phi_s^{\text{SM}} = 2\arg(V_{ts}^*V_{tb}) = -2\lambda^2\eta = -(2.08 \pm 0.09)^\circ, \quad (6)$$

where  $\lambda \equiv |V_{us}|$  and  $\eta$  (measuring the height of the unitarity triangle) are Wolfenstein parameters [53], and the numerical value refers to the analysis of the CKM matrix performed in Refs. [54, 55]. For a detailed discussion of the formalism of  $B_s^0$ – $\bar{B}_s^0$  mixing, the reader is referred to [56].

In the presence of NP, new particles may enter the box diagram (as illustrated in the right panel of Fig. 2), or may give rise to new contributions at the tree level, which is forbidden in the SM. Should new CP-violating phases be involved, they would manifest themselves through the  $\phi_s^{\text{NP}}$  term in (5), which could then make  $\phi_s$  differ sizably from its SM value (see, for instance, Refs. [57]–[60] and references therein).

Another characteristic feature of the  $B_s$ -meson system is the decay width difference  $\Delta\Gamma_s$ . Thanks to  $b \rightarrow c\bar{c}s$  quark-level processes, it is expected to be sizable in the SM [61, 62], with  $\Delta\Gamma_s/\Gamma_s|_{\text{SM}} \sim 0.15$ , while the counterpart of this quantity for the  $B_d$ -meson system is expected at the 0.1% level. The current situation has recently been summarized in Ref. [63].

## 2.2 $B_s^0$ – $\bar{B}_s^0$ Oscillations

Since the first observation of particle–antiparticle transformations in neutral  $B$  mesons in 1987 [64], the determination of the  $B_s^0$ – $\bar{B}_s^0$  oscillation frequency  $\Delta M_s$  from a time-dependent measurement of  $B_s^0$ – $\bar{B}_s^0$  oscillations has been a major objective of experimental particle physics. A long standing search was performed during more than 19 years, mainly due to the fact that the  $B_s^0$ – $\bar{B}_s^0$  oscillation frequency is 35 times larger than that for the  $B_d^0$ – $\bar{B}_d^0$  system, posing a considerable challenge for the decay time resolution of the detectors. The large statistics available at the Tevatron and the good proper time reconstruction allowed in 2006 the DØ and CDF experiments to produce the first precise measurements [65, 66]. More recently, with only  $36 \text{ pb}^{-1}$ , the LHCb experiment has confirmed the measurement with a similar statistical precision but a smaller systematical uncertainty [67]. The  $B_s^0$ – $\bar{B}_s^0$  mixing frequency is now known with a precision better than 0.5 % [68] :

$$\Delta M_s = (17.69 \pm 0.08) \text{ ps}^{-1} \quad (7)$$



Note that the ability to resolve these fast  $B_s^0-\bar{B}_s^0$  oscillations is a prerequisite for many physics analyses. In particular it is essential for the study of the time-dependent CP asymmetry of  $B_s^0 \rightarrow J/\psi\phi$ .

The mass difference  $\Delta M_s$  is proportional to the CKM coefficient  $|V_{ts}|^2$ . However, the value of  $|V_{ts}|$  directly extracted from  $\Delta M_s$  has large theoretical uncertainties related to the contribution of non-perturbative QCD effects. Many such uncertainties cancel in the ratio  $\Delta M_s/\Delta M_d$ , which can be expressed as

$$\frac{\Delta M_s}{\Delta M_d} = \xi^2 \frac{M_{B_s^0}}{M_{B_d^0}} \left| \frac{V_{ts}}{V_{td}} \right|^2. \quad (8)$$

Here  $\xi$  is an  $SU(3)$  flavor-symmetry-breaking factor, while the  $M_{B_q^0}$  denote the masses of the  $B_q^0$  mesons. The former non-perturbative parameter can be determined with the help lattice QCD, where the most recent value reads as follows [69]:

$$\xi = 1.237 \pm 0.032. \quad (9)$$

Using this result and the average of the  $\Delta M_s$  measurements by the CDF and LHCb experiments, the value

$$\left| \frac{V_{ts}}{V_{td}} \right| = 0.2111 \pm 0.0010(\text{exp}) \pm 0.0055(\text{lattice}) \quad (10)$$

has been extracted [68]. It can be seen that the theoretical uncertainties still dominate in this ratio. They need to be improved in the future for a precise test of the unitarity relation of the CKM matrix.

### 2.3 Untagged $B_s$ Decay Rates and Branching Ratios

A particularly interesting case arises if no distinction, i.e. “tagging”, is made between initially present  $B_s^0$  or  $\bar{B}_s^0$  mesons. The corresponding “untagged” decay rate is a sum of two exponentials:

$$\langle \Gamma(B_s(t) \rightarrow f) \rangle \equiv \Gamma(B_s^0(t) \rightarrow f) + \Gamma(\bar{B}_s^0(t) \rightarrow f) = R_{\text{H}}^f e^{-\Gamma_{\text{H}}^{(s)} t} + R_{\text{L}}^f e^{-\Gamma_{\text{L}}^{(s)} t}. \quad (11)$$

This expression can be rewritten as

$$\langle \Gamma(B_s(t) \rightarrow f) \rangle = \left( R_{\text{H}}^f + R_{\text{L}}^f \right) e^{-\Gamma_s t} \left[ \cosh(y_s t / \tau_{B_s}) + \mathcal{A}_{\Delta\Gamma}^f \sinh(y_s t / \tau_{B_s}) \right], \quad (12)$$

where the observable

$$\mathcal{A}_{\Delta\Gamma}^f \equiv \frac{R_{\text{H}}^f - R_{\text{L}}^f}{R_{\text{H}}^f + R_{\text{L}}^f} \quad (13)$$

depends on the final state  $f$ , and

$$y_s \equiv \frac{\Delta\Gamma_s}{2\Gamma_s} \equiv \frac{\Gamma_{\text{L}}^{(s)} - \Gamma_{\text{H}}^{(s)}}{2\Gamma_s} = 0.088 \pm 0.014 \quad (14)$$

describes the impact of a non-vanishing decay width difference  $\Delta\Gamma_s$ ; the average decay width

$$\Gamma_s \equiv \frac{\Gamma_L^{(s)} + \Gamma_H^{(s)}}{2\Gamma_s} = \tau_{B_s}^{-1} = (0.6580 \pm 0.0085) \text{ ps}^{-1} \quad (15)$$

is given by the inverse of the  $B_s$  lifetime  $\tau_{B_s}$ . The numerical values in (14) and (15) correspond to the results reported in Ref. [70].

The untagged rates (12) are used by experiments for the extraction of branching ratios. However, usually no time information for the untagged data sample is taken into account, which corresponds to the following time-integrated, ‘‘experimental’’ branching ratios [40, 71]:

$$\begin{aligned} \text{BR}(B_s \rightarrow f)_{\text{exp}} &\equiv \frac{1}{2} \int_0^\infty \langle \Gamma(B_s(t) \rightarrow f) \rangle dt \\ &= \frac{1}{2} \left[ \frac{R_H^f}{\Gamma_H^{(s)}} + \frac{R_L^f}{\Gamma_L^{(s)}} \right] = \frac{\tau_{B_s}}{2} (R_H^f + R_L^f) \left[ \frac{1 + \mathcal{A}_{\Delta\Gamma}^f y_s}{1 - y_s^2} \right]. \end{aligned} \quad (16)$$

On the other hand, in the theory community, the  $B_s^0$ - $\bar{B}_s^0$  oscillations are usually ‘‘switched off’’ by choosing  $t = 0$ , and the following CP-averaged branching ratios are calculated:

$$\text{BR}(B_s \rightarrow f)_{\text{theo}} \equiv \frac{\tau_{B_s}}{2} \langle \Gamma(B_s^0(t) \rightarrow f) \rangle \Big|_{t=0} = \frac{\tau_{B_s}}{2} (R_H^f + R_L^f). \quad (17)$$

The advantage of this  $B_s$  branching ratio concept is the possibility of comparing straightforwardly with branching ratios of decays of  $B_d^0$  or  $B_u^+$  mesons that are related to one another by the  $SU(3)_F$  flavor symmetry of strong interactions.

The conversion between the time-integrated and theoretical branching ratios defined in (16) and (17), respectively, can be accomplished with the help of the following relation [40]:

$$\text{BR}(B_s \rightarrow f)_{\text{theo}} = \left[ \frac{1 - y_s^2}{1 + \mathcal{A}_{\Delta\Gamma}^f y_s} \right] \text{BR}(B_s \rightarrow f)_{\text{exp}}. \quad (18)$$

While the term in square brackets would be equal to one in the presence of a vanishing decay width difference  $\Delta\Gamma_s$ , the experimental value of  $y_s$  in (14) can lead to a difference between theoretical  $B_s \rightarrow f$  branching ratios and their experimental counterparts as large as 10%, depending on the final state  $f$ . A compilation of these effects, based on theoretical analyses which make in particular use of the  $SU(3)$  flavor symmetry, can be found in Ref. [40]. Subtleties related to  $\Delta\Gamma_s$  in the experimental analysis of the  $B_s \rightarrow K^{*0} \bar{K}^{*0}$  channel were also discussed in Refs. [72, 73].

## 2.4 Effective $B_s$ Decay Lifetimes

The theoretical input for the conversion of the branching ratios into the corresponding theoretical branching ratios can be avoided as soon as time information for the untagged  $B_s$  data is available. In this case, the effective  $B_s$  lifetime of the decay at hand [74], which is defined as

$$\tau_f \equiv \frac{\int_0^\infty t \langle \Gamma(B_s(t) \rightarrow f) \rangle dt}{\int_0^\infty \langle \Gamma(B_s(t) \rightarrow f) \rangle dt} = \frac{\tau_{B_s}}{1 - y_s^2} \left[ \frac{1 + 2 \mathcal{A}_{\Delta\Gamma}^f y_s + y_s^2}{1 + \mathcal{A}_{\Delta\Gamma}^f y_s} \right], \quad (19)$$

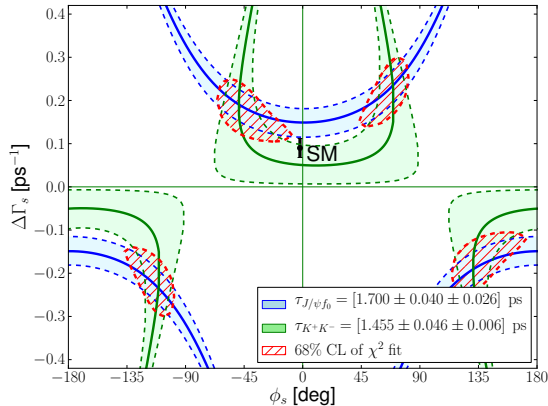


Figure 3: Constraints in the  $\phi_s - \Delta\Gamma_s$  plane from measurements of the effective lifetimes of the  $B_s^0 \rightarrow K^+K^-$  and  $B_s^0 \rightarrow J/\psi f_0$  decays [74, 75].

can be extracted, thereby yielding the following expression [40]:

$$\text{BR}(B_s \rightarrow f)_{\text{theo}} = \left[ 2 - (1 - y_s^2) \frac{\tau_f}{\tau_{B_s}} \right] \text{BR}(B_s \rightarrow f)_{\text{exp}}; \quad (20)$$

it should be emphasized that only measurable quantities appear on the right-hand side. The measurement of effective  $B_s$  decay lifetimes is hence an integral part of the extraction of the theoretical branching ratios (17) from the data.

Another interesting application of effective lifetimes of  $B_s$  decays is that they allow us to probe the CP-violating mixing phase  $\phi_s$  and the decay width difference  $\Delta\Gamma_s$ . In particular, the lifetimes can be converted into contours in the  $\phi_s - \Delta\Gamma_s$  plane, where the intersection of the contours related to the effective lifetimes of  $B_s$  decays into CP-even (such as  $B_s \rightarrow K^+K^-$ ) and CP-odd (such as  $B_s \rightarrow J/\psi f_0$  with  $f_0 \equiv f_0(980)$ ) final states allows the extraction of  $\phi_s$  and  $\Delta\Gamma_s$  [74, 75]. This determination is extremely robust with respect to the hadronic penguin uncertainties and complements nicely studies of CP violation in  $B_s^0 \rightarrow J/\psi\phi$  and  $B_s^0 \rightarrow J/\psi f_0$  decays to be discussed in Section 3.

The first measurements of effective lifetimes for  $B_s$  decays into final CP eigenstates by the CDF and LHCb collaborations have recently become available. The LHCb collaboration measured the effective lifetime of the  $B_s^0 \rightarrow K^+K^-$  decay and published two independent results [36, 37] using the statistics collected in 2010 and 2011:

$$\tau_{K^+K^-} = [1.440 \pm 0.096(\text{stat}) \pm 0.009(\text{syst})] \text{ ps } (37 \text{ pb}^{-1}), \quad (21)$$

$$\tau_{K^+K^-} = [1.455 \pm 0.046(\text{stat}) \pm 0.006(\text{syst})] \text{ ps } (1 \text{ fb}^{-1}). \quad (22)$$

The  $B_s^0$  lifetime in the decay mode  $B_s^0 \rightarrow J/\psi f_0(980)$  with  $f_0(980) \rightarrow \pi^+\pi^-$  was measured by the CDF and LHCb collaborations. The CDF collaboration has analyzed  $3.7 \text{ fb}^{-1}$  and reconstructed  $502 \pm 37$  such decays and has found [38]

$$\tau_{J/\psi f_0} = [1.70_{-0.11}^{+0.12}(\text{stat}) \pm 0.03(\text{syst})] \text{ ps}. \quad (23)$$

The LHCb collaboration has reconstructed  $4040 \pm 75$  decays  $B_s^0 \rightarrow J/\psi f_0$  using the statistics corresponding to the integrated luminosity of  $1 \text{ fb}^{-1}$  and has obtained [39]

$$\tau_{J/\psi f_0} = [1.700 \pm 0.040(\text{stat}) \pm 0.026(\text{syst})] \text{ ps}. \quad (24)$$

The results (23) and (24) are in very good agreement, although with a better precision for the LHCb result. It is important to note that the difference between the  $B_s^0$  lifetime in the decay modes  $B_s^0 \rightarrow K^+ K^-$  and  $B_s^0 \rightarrow J/\psi f_0(980)$  exceeds three standard deviation, which is an independent evidence of the non-zero decay width difference  $\Delta\Gamma_s$  of the  $B_s$ -meson system.

In Fig. 3, we show the constraints in the  $\phi_s - \Delta\Gamma_s$  plane that follow from the effective  $B_s^0$  decay lifetime measurements discussed above. Future lifetime measurements with 1% uncertainty would be most interesting.

## 3 CP Violation in $B_s^0$ Decays

### 3.1 Introduction

Decays of  $B_s^0$  mesons allow interesting studies of CP violation. In the analyses of the corresponding CP-violating rate asymmetries it is essential that “tagging” information is available, allowing the distinction between initially present  $B_s^0$  or  $\bar{B}_s^0$  meson states. Let us, for simplicity, consider a decay into a CP eigenstate  $f$ , which will also be particularly relevant for the major part of the discussion in this section. The CP-violating rate asymmetry takes then the following form:

$$\frac{\Gamma(B_s^0(t) \rightarrow f) - \Gamma(\bar{B}_s^0(t) \rightarrow f)}{\Gamma(B_s^0(t) \rightarrow f) + \Gamma(\bar{B}_s^0(t) \rightarrow f)} = \frac{C(B_s \rightarrow f) \cos(\Delta M_s t) - S(B_s \rightarrow f) \sin(\Delta M_s t)}{\cosh(\Delta\Gamma_s t/2) + \mathcal{A}_{\Delta\Gamma}(B_s \rightarrow f) \sinh(\Delta\Gamma_s t/2)}, \quad (25)$$

where the the time-dependent rates refer to initially present  $B_s^0$  or  $\bar{B}_s^0$  states.

The observable  $C(B_s \rightarrow f)$  describes “direct” CP violation, which is caused by the interference between different amplitudes contributing to the decay at hand, with non-trivial CP-conserving strong and CP-violating weak phase differences. On the other hand, the observable  $S(B_s \rightarrow f)$  originates from interference between  $B_s^0 - \bar{B}_s^0$  mixing and  $B_s^0, \bar{B}_s^0 \rightarrow f$  decay processes and is referred to as “mixing-induced” CP violation. The observable  $\mathcal{A}_{\Delta\Gamma}(B_s \rightarrow f)$  arises in the untagged rate, as we have already discussed in (12). It should be noted that these observables are not independent from one another, satisfying the following relation:

$$[C(B_s \rightarrow f)]^2 + [S(B_s \rightarrow f)]^2 + [\mathcal{A}_{\Delta\Gamma}(B_s \rightarrow f)]^2 = 1. \quad (26)$$

For a detailed discussion of the calculation of these observables, the reader is referred to [56].

In the rate asymmetry in Eq. (25), CP violation in  $B_s^0 - \bar{B}_s^0$  oscillations has been neglected as this phenomenon has here a tiny impact. Before turning to  $B_s^0 \rightarrow J/\psi \phi$ , which is one of the most prominent  $B_s^0$ -meson decays to explore CP violation, let us first have a closer look at CP violation in  $B_s^0 - \bar{B}_s^0$  mixing.

### 3.2 CP Violation in $B_s^0-\bar{B}_s^0$ Mixing

CP violation in the mixing of the neutral  $B_q^0$  mesons ( $q = d, s$ ) is described by the phase  $\phi_{12}^q$ , which is defined as

$$\phi_{12}^q \equiv \arg \left( -\frac{M_{12}^q}{\Gamma_{12}^q} \right). \quad (27)$$

The phase  $\phi_{12}^s$  should not be mixed up with the  $\phi_s$  introduced in (5). In the presence of NP contributions to  $B_s^0-\bar{B}_s^0$  mixing, it takes the form

$$\phi_{12}^s = \phi_{12}^s|_{\text{SM}} + \phi_s^{\text{NP}}, \quad (28)$$

where the SM piece takes the following numerical value [61]:

$$\phi_{12}^s|_{\text{SM}} = (0.22 \pm 0.06)^\circ, \quad (29)$$

and  $\phi_s^{\text{NP}}$  is the same NP phase entering also (5). The notation agrees with that of Ref. [76].

The parameters  $M_{12}^q$  and  $\Gamma_{12}^q$  are the complex non-diagonal elements of the mass mixing matrix. They are related to the observable quantities  $\Delta M_q$  and  $\Delta\Gamma_q$  introduced in (4) as

$$\Delta M_q = 2 |M_{12}^q|, \quad \Delta\Gamma_q = 2 |\Gamma_{12}^q| \cos \phi_{12}^q, \quad (30)$$

where it should be emphasized that  $\phi_{12}^q$  enters the decay width difference [77]. The CP-violating phase  $\phi_{12}^q$  can be extracted from the charge asymmetry  $a_{\text{sl}}^q$  for “wrong-charge” semileptonic  $B_q^0$ -meson decays induced by oscillations, which is defined as

$$a_{\text{sl}}^q = \frac{\Gamma(\bar{B}_q^0(t) \rightarrow \ell^+ X) - \Gamma(B_q^0(t) \rightarrow \ell^- X)}{\Gamma(\bar{B}_q^0(t) \rightarrow \ell^+ X) + \Gamma(B_q^0(t) \rightarrow \ell^- X)}. \quad (31)$$

This quantity is independent of the decay time  $t$ , and can be expressed as

$$a_{\text{sl}}^q = \left| \frac{\Gamma_{12}^q}{M_{12}^q} \right| \sin \phi_{12}^q = \frac{\Delta\Gamma_q}{\Delta M_q} \tan \phi_{12}^q. \quad (32)$$

For a much more detailed discussion of this topic, we refer the reader to Ref. [63].

In experimental measurements, the muon is much easier to identify than any other lepton. Therefore all experimental results on the semileptonic charge asymmetry are obtained with  $\ell = \mu$  in Eq. (31). The SM predicts values of  $a_{\text{sl}}^d$  and  $a_{\text{sl}}^s$  which are not detectable with the current experimental precision [61]:

$$a_{\text{sl}}^d|_{\text{SM}} = -(4.1 \pm 0.6) \times 10^{-4}, \quad a_{\text{sl}}^s|_{\text{SM}} = (1.9 \pm 0.3) \times 10^{-5}. \quad (33)$$

Additional contributions to CP violation via loop diagrams appear in some extensions of the SM [78–83] and can result in these asymmetries within experimental reach.

The DØ experiment performed several measurements of the semileptonic  $B_d^0$  and  $B_s^0$  charge asymmetry. The polarities of the toroidal and solenoidal magnetic fields of DØ detector were regularly reversed so that the four solenoid-toroid polarity combinations were exposed to approximately the same integrated luminosity. This feature is especially

important in the measurements of the charge asymmetry, because the reversal of magnets polarities allows for a cancellation of first order effects related with the instrumental asymmetry and the reduction of the corresponding systematic uncertainty.

One of the  $D\bar{O}$  results [13] consists in measuring the like-sign dimuon charge asymmetry  $A_{\text{sl}}^b$ . Assuming that this asymmetry is produced by CP violation in the mixing of the  $B_d^0$  and  $B_s^0$  mesons, it can be expressed as

$$A_{\text{sl}}^b = C_d a_{\text{sl}}^d + C_s a_{\text{sl}}^s, \quad (34)$$

where the coefficients  $C_d$  and  $C_s$  depend on the mean mixing probabilities  $\chi_d$  and  $\chi_s$  and the production rates of the  $B_d^0$  and  $B_s^0$  mesons. Using the integrated luminosity of  $9.1 \text{ fb}^{-1}$ , the  $D\bar{O}$  experiment obtained

$$A_{\text{sl}}^b = [-0.787 \pm 0.172(\text{stat}) \pm 0.093(\text{syst})]\%. \quad (35)$$

This result differs by 3.9 standard deviation from the SM prediction [61]:

$$A_{\text{sl}}^b|_{\text{SM}} = (-2.3 \pm 0.4) \times 10^{-4}. \quad (36)$$

From the study of the impact parameter dependence of the asymmetry, the  $D\bar{O}$  experiment extracted separate values of  $a_{\text{sl}}^d$  and  $a_{\text{sl}}^s$

$$\begin{aligned} a_{\text{sl}}^d &= (-0.12 \pm 0.52)\%, \\ a_{\text{sl}}^s &= (-1.81 \pm 1.06)\%. \end{aligned} \quad (37)$$

The correlation  $\rho_{ds}$  between these two quantities is

$$\rho_{ds} = -0.799. \quad (38)$$

The  $D\bar{O}$  experiment also performed separate measurements of the asymmetries  $a_{\text{sl}}^d$  and  $a_{\text{sl}}^s$  using the semileptonic decays  $B_d^0 \rightarrow \mu^+ \nu D^- X$ ,  $B_d^0 \rightarrow \mu^+ \mu D^{*-} X$  [14], and  $B_s^0 \rightarrow \mu^+ \nu D_s^- X$  [15], respectively. They obtained the following values:

$$a_{\text{sl}}^d = [+0.68 \pm 0.45(\text{stat}) \pm 0.14(\text{syst})]\%, \quad (39)$$

$$a_{\text{sl}}^s = [-1.08 \pm 0.72(\text{stat}) \pm 0.17(\text{syst})]\%. \quad (40)$$

Recently, the LHCb collaboration has performed a similar measurement [16] of the asymmetry  $a_{\text{sl}}^s$  using the decays  $B_s^0 \rightarrow \mu^+ \nu D_s^- X$  and has obtained the most precise value to date :

$$a_{\text{sl}}^s = [-0.24 \pm 0.54(\text{stat}) \pm 0.33(\text{syst})]\%. \quad (41)$$

All these results are consistent with one another, although the LHCb measurement does not confirm the significant deviation from the SM observed by the  $D\bar{O}$  experiment. The  $a_{\text{sl}}^d$  asymmetry has also been measured at B-factories with a very good accuracy [84] :

$$a_{\text{sl}}^d = (0.02 \pm 0.31)\% \quad (42)$$

Putting everything together, the deviation from the SM is significantly reduced to 2.4 standard deviations [84]. However, the current size of the experimental uncertainties still allows for possible NP contributions.

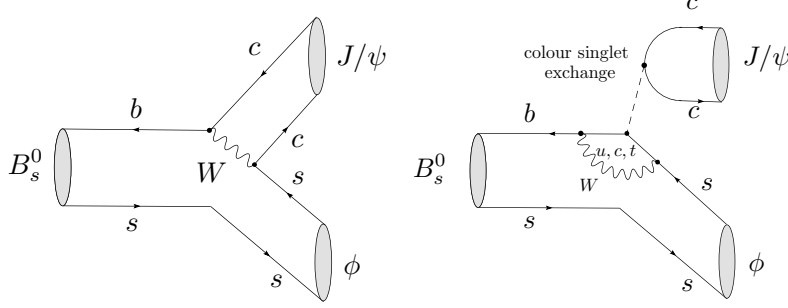


Figure 4: Decay topologies contributing to the  $B_s^0 \rightarrow J/\psi\phi$  decay in the SM.

### 3.3 CP Violation in $B_s^0 \rightarrow J/\psi\phi$

The most prominent  $B_s^0$ -meson decay to explore CP violation is the  $B_s^0 \rightarrow J/\psi\phi$  channel. It is the  $B_s^0$  counterpart of the  $B_d^0 \rightarrow J/\psi K_S$  decay, which was in the main focus of the  $B$  factories in the previous decade and has allowed the BaBar and Belle collaborations to establish CP violation in the  $B_d^0$  system. In the SM, the CP-violating asymmetry is proportional to  $\sin 2\beta$ , where  $\beta = \arg(-V_{cd}V_{cb}^*/V_{td}V_{tb}^*)$  denotes the usual angle of the CKM unitarity triangle.

In the case of  $B_s^0 \rightarrow J/\psi\phi$ , CP-violating effects allow us to probe the CP-violating  $B_s^0$ - $B_s^0$  mixing phase  $\phi_s$ , which was introduced in (5) and takes the tiny SM value given in (6). Since the final state involves two vector mesons which can be present in final state configurations  $f \in \{0, \parallel, \perp\}$  [85], we have to deal with a mixture of CP-even and CP-odd eigenstates. For the extraction of  $\phi_s$ , these CP eigenstates have to be disentangled, which can be accomplished with the help of a time-dependent angular analysis of the  $J/\psi \rightarrow \mu^+\mu^-$  and  $\phi \rightarrow K^+K^-$  decay products [86, 87].

In the SM, the  $B_s^0 \rightarrow J/\psi\phi$  decay receives contributions from color-suppressed tree and penguin topologies, as illustrated in Fig. 4. For a given final-state configuration  $f$ , the corresponding transition amplitude can be written as follows [26]:

$$A(B_s^0 \rightarrow (J/\psi\phi)_f) = (1 - \lambda^2/2) \mathcal{A}'_f \left[ 1 + \epsilon a'_f e^{i\theta'_f} e^{i\gamma} \right], \quad (43)$$

where the following CP-conserving parameters enter:

$$\mathcal{A}'_f \equiv \lambda^2 A \left[ A_{T,f}^{(c)'} + A_{P,f}^{(c)'} - A_{P,f}^{(t)'} \right], \quad a'_f e^{i\theta'_f} \equiv R_b \left[ \frac{A_{P,f}^{(u)'} - A_{P,f}^{(t)'}}{A_{T,f}^{(c)'} + A_{P,f}^{(c)'} - A_{P,f}^{(t)'}} \right]. \quad (44)$$

Here  $A_{T,f}^{(c)'}$  is the color-suppressed tree contribution and the  $A_{P,f}^{(q)'}$  denote penguin topologies with internal  $q$  quarks shown in Fig. 4. The primes are a reminder that we are dealing with a  $\bar{b} \rightarrow \bar{c}c\bar{s}$  transition. Moreover, the decay amplitude involves the CKM factors

$$A \equiv \frac{1}{\lambda^2} |V_{cb}| \sim 0.8, \quad R_b \equiv \left( 1 - \frac{\lambda^2}{2} \right) \frac{1}{\lambda} \left| \frac{V_{ub}}{V_{cb}} \right| \sim 0.5, \quad \epsilon \equiv \frac{\lambda^2}{1 - \lambda^2} = 0.053. \quad (45)$$

The parameters in (44) suffer from large hadronic uncertainties, in particular the  $a'_f e^{i\theta'_f}$ , which is a measure of the ratio of the tree to penguin contributions. However, as the

latter quantity is doubly Cabibbo-suppressed in (43) by the tiny  $\epsilon$  parameter, it is usually neglected.

The angular analysis allows to construct CP asymmetries in analogy to (25) for the final-state configurations  $f \in \{0, \parallel, \perp\}$ , where the CP-violating observables can be written as follows [26]:

$$C(B_s \rightarrow (J/\psi\phi)_f) = -\frac{2\epsilon a'_f \sin \theta'_f \sin \gamma}{1 + 2\epsilon a'_f \cos \theta'_f \cos \gamma + \epsilon^2 a_f'^2} \quad (46)$$

$$\frac{S(B_s \rightarrow (J/\psi\phi)_f)}{\sqrt{1 - C(B_s \rightarrow (J/\psi\phi)_f)^2}} = \sin(\phi_s + \Delta\phi_s^f). \quad (47)$$

Here the  $\Delta\phi_s^f$  denotes a hadronic phase shift, which is given by

$$\tan \Delta\phi_s^f = \frac{2\epsilon a'_f \cos \theta'_f \sin \gamma + \epsilon^2 a_f'^2 \sin 2\gamma}{1 + 2\epsilon a'_f \cos \theta'_f \cos \gamma + \epsilon^2 a_f'^2 \cos 2\gamma}. \quad (48)$$

Using data for direct CP violation in  $B_d \rightarrow J/\psi K_S$ , the correction due to the square root in (47) is tiny, so that this expression can be simplified as

$$S(B_s \rightarrow (J/\psi\phi)_f) = \sin(\phi_s + \Delta\phi_s^f). \quad (49)$$

In the literature, it is usually assumed that  $\Delta\phi_s^f = 0$ . Making this assumption, HFAG has compiled the most recent average  $\phi_s = -(0.74_{-4.8}^{+5.2})^\circ$  [88], which is fully consistent with the SM value in (6). Once the experimental precision improves further, even a small phase shift  $\Delta\phi_s^f$  at the  $1^\circ$  level may have a significant impact on the extraction of  $\phi_s$  from (49) and the resolution of possible CP-violating NP contributions to  $B_s^0\text{-}\bar{B}_s^0$  mixing.

A channel to probe these penguin contributions is offered by  $B_s^0 \rightarrow J/\psi \bar{K}^{*0}$ , with a SM decay amplitude of the structure

$$A(B_s^0 \rightarrow (J/\psi \bar{K}^{*0})_f) = -\lambda \mathcal{A}_f [1 - a_f e^{i\theta_f} e^{i\gamma}]. \quad (50)$$

The key feature is that here the  $a_f e^{i\theta_f}$  term is not suppressed by the tiny  $\epsilon$  parameter. Neglecting penguin annihilation ( $PA$ ) and exchange topologies ( $E$ ), which can be constrained by the upper bound on  $\text{BR}(B_d \rightarrow J/\psi\phi)$  as  $|E + PA|/|T| \lesssim 0.1$ , and using the  $SU(3)$  flavor symmetry, we get the relations  $a_f = a'_f$  and  $\theta_f = \theta'_f$ , allowing us to get a handle on the penguin shift  $\Delta\phi_s^f$  [26].

Since  $B_s^0 \rightarrow J/\psi \bar{K}^{*0}$  is a flavor-specific decay and does not exhibit mixing-induced CP violation, the implementation of this method has to use measurements of untagged and direct CP-violating observables, and an angular analysis is required to disentangle the final-state configurations  $f$ .

The experimental measurement of CP violation in  $B_s^0 \rightarrow J/\psi\phi$  decays has been pioneered by the CDF and DØ collaborations. Both these experiments reported their final study of this channel with the full statistics. The CDF collaboration [17] reconstructs about 11000 such decays using the integrated luminosity  $9.6 \text{ fb}^{-1}$ . The obtained



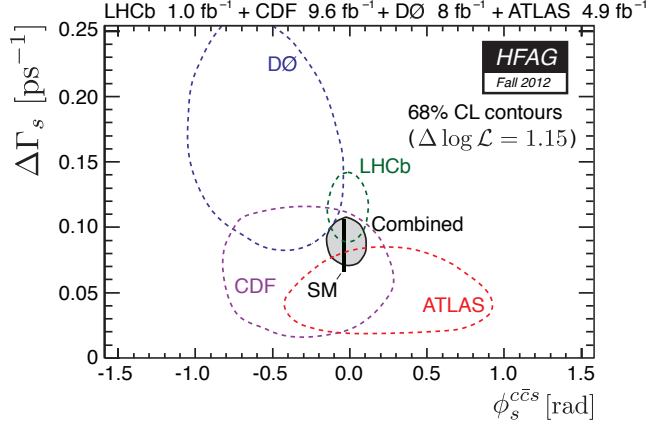


Figure 5: Constraints of all measurements of CP violation in the  $B_s^0 \rightarrow J/\psi\phi$  decay in the  $\phi_s$ - $\Delta\Gamma_s$  plane (from Ref. [84]).

confidence regions for the quantity  $\beta_s \equiv -\phi_s/2$  is

$$\beta_s \in [-\pi/2, -1.51] \cup [-0.06, 0.30] \cup [1.26, \pi/2] \text{ (68\% C.L.)}, \quad (51)$$

$$\beta_s \in [-\pi/2, -1.36] \cup [-0.21, 0.53] \cup [1.04, \pi/2] \text{ (95\% C.L.)}. \quad (52)$$

Assuming the SM value for the CP-violating phase  $\beta_s$ , the CDF collaboration measured

$$\tau_s = [1.528 \pm 0.019 \text{ (stat)} \pm 0.009 \text{ (syst)}] \text{ ps}, \quad (53)$$

$$\Delta\Gamma_s = [0.068 \pm 0.026 \text{ (stat)} \pm 0.009 \text{ (syst)}] \text{ ps}^{-1}. \quad (54)$$

A similar analysis by the DØ collaboration [18] is based on 6500 signal events collected using the integrated luminosity  $8 \text{ fb}^{-1}$ . The result is consistent with the SM prediction:

$$\begin{aligned} \tau_s &= [1.443^{+0.038}_{-0.035}] \text{ ps}, \\ \Delta\Gamma_s &= [0.163^{+0.065}_{-0.064}] \text{ ps}^{-1}, \\ \phi_s &= -0.55^{+0.38}_{-0.36}. \end{aligned} \quad (55)$$

Recently the LHCb experiment reported [19] the most precise analysis of such measurement. Using a data sample of  $0.37 \text{ fb}^{-1}$ , they obtained

$$\Gamma_s = [0.657 \pm 0.009 \text{ (stat)} \pm 0.008 \text{ (syst)}] \text{ ps}^{-1}, \quad (56)$$

$$\Delta\Gamma_s = [0.123 \pm 0.029 \text{ (stat)} \pm 0.011 \text{ (syst)}] \text{ ps}^{-1}, \quad (57)$$

$$\phi_s = 0.15 \pm 0.18 \text{ (stat)} \pm 0.06 \text{ (syst)}. \quad (58)$$

Finally, the ATLAS experiment also performed a study of this final state [20], reporting the following results:

$$\Gamma_s = [0.677 \pm 0.007 \text{ (stat)} \pm 0.004 \text{ (syst)}] \text{ ps}^{-1}, \quad (59)$$

$$\Delta\Gamma_s = [0.053 \pm 0.021 \text{ (stat)} \pm 0.010 \text{ (syst)}] \text{ ps}^{-1}, \quad (60)$$

$$\phi_s = 0.22 \pm 0.41 \text{ (stat)} \pm 0.10 \text{ (syst)}. \quad (61)$$

The combination of all measurements of CP violation in  $B_s^0 \rightarrow J/\psi\phi$  is shown in Fig. 5 taken from [84]. Since the time-dependent differential decay rates describing the decay  $B_s^0 \rightarrow J/\psi\phi$  are invariant under the transformation  $(\phi_s, \Delta\Gamma_s) \leftrightarrow (\pi - \phi_s, -\Delta\Gamma_s)$ , together with an appropriate transformation for the strong phases, two solutions are allowed. This ambiguity can be resolved using the decay  $B_s^0 \rightarrow J/\psi K^+ K^-$  [89]. The total decay amplitude is a coherent sum of a slowly varying S-wave (either due to the  $f_0(980)$  or a non-resonant contribution) and a P-wave varying rapidly in the  $\phi(1020)$  mass region. By measuring this phase difference as a function of the  $K^+ K^-$  invariant mass, the LHCb collaboration has been able to resolve this ambiguity [90]: the sign of  $\Delta\Gamma_s$  is determined to be positive, as predicted in the SM.

The  $B_s^0 \rightarrow J/\psi \bar{K}^{*0}$  decay was observed by CDF [91] and LHCb [92]. The most recent LHCb branching ratio  $(4.4_{-0.4}^{+0.5} \pm 0.8) \times 10^{-5}$  agrees well with the prediction  $(4.6 \pm 0.4) \times 10^{-5}$  obtained from the  $\text{BR}(B_d^0 \rightarrow J/\psi \rho^0)$  by means of the  $SU(3)$  flavor symmetry [26], and the polarization fractions agree well with those of  $B_d^0 \rightarrow J/\psi K^{*0}$ .

The experimental sensitivity for the extraction of  $\phi_s$  from  $B_s^0 \rightarrow J/\psi\phi$  at the LHCb upgrade ( $50 \text{ fb}^{-1}$ ) is expected as  $\Delta\phi_s|_{\text{exp}} \sim 0.008 = 0.46^\circ$  [76]. In view of this impressive precision on the one hand and  $\Delta\phi_d = -(1.28 \pm 0.74)^\circ$  following from the current data for  $B_d^0 \rightarrow J/\psi\pi, J/\psi K$  decays with a dynamics similar to  $B_s^0 \rightarrow J/\psi\phi$  on the other hand [93], it will be crucial to get a handle on the penguin effects at the LHCb upgrade as they may mimic NP effects.

### 3.4 CP Violation in $B_s^0 \rightarrow J/\psi f_0(980)$

Another  $B_s^0$ -meson decay which has recently entered the stage is  $B_s^0 \rightarrow J/\psi f_0(980)$ . This channel was observed by the LHCb [94], Belle [95], CDF [96] and DØ [97] collaborations. The dominant decay mode proceeds via  $f_0 \rightarrow \pi^+ \pi^-$ , with a branching ratio about four times smaller than that of  $B_s^0 \rightarrow J/\psi\phi$  with  $\phi \rightarrow K^+ K^-$ . On the other hand, since the  $f_0 \equiv f_0(980)$  is a scalar  $J^{PC} = 0^{++}$  state, the final state is CP-odd so that no angular analysis is required in order to disentangle CP eigenstates as in the case of the  $B_s^0 \rightarrow J/\psi\phi$  decay. Consequently, the analysis is simplified considerably and offers an interesting alternative for the determination of  $\phi_s$  [98, 99].

The impact of hadronic uncertainties on the extraction of  $\phi_s$  from CP violation in  $B_s^0 \rightarrow J/\psi f_0$  was studied in detail in [28], and for the  $B_{s,d} \rightarrow J/\psi \eta^{(\prime)}$  system in [29]. The general formalism is analogous to the discussion in Subsection 3.3:

$$A(B_s^0 \rightarrow J/\psi f_0) \propto [1 + \epsilon b e^{i\vartheta} e^{i\gamma}]. \quad (62)$$

The key feature is again that the hadronic penguin parameters is doubly Cabibbo-suppressed by the tiny  $\epsilon$ . The mixing-induced CP asymmetry can be written as

$$S(B_s^0 \rightarrow J/\psi f_0) = \sqrt{1 - C(B_s^0 \rightarrow J/\psi f_0)^2} \sin(\phi_s + \Delta\tilde{\phi}_s), \quad (63)$$

where  $\Delta\tilde{\phi}_s$  is given by an expression analogous to (48). However, in contrast to the  $B_d^0 \rightarrow J/\psi K_S$  and  $B_s^0 \rightarrow J/\psi\phi$  decays, the  $B_s^0 \rightarrow J/\psi f_0$  channel suffers from the fact that the hadronic structure of the  $f_0(980)$  is poorly known: popular benchmark scenarios are the quark-antiquark and tetraquark pictures. In the latter case, a peculiar decay

topology arises at the tree level that does not have a counterpart in the quark–antiquark description [28].

The parameter  $b$  depends on the hadronic composition of the  $f_0$  and is therefore essentially unknown. Making the conservative assumption  $0 \leq b \leq 0.5$  (where the upper bound of 0.5 is related to the  $R_b \sim 0.5$  factor in (44)) and  $0^\circ \leq \vartheta \leq 360^\circ$  yields  $\Delta\tilde{\phi}_s \in [-2.9^\circ, 2.8^\circ]$ . This range translates into the SM range

$$S(B_s \rightarrow J/\psi f_0)|_{\text{SM}} \in [-0.086, -0.012], \quad (64)$$

while the naive value with  $\Delta\tilde{\phi}_s = 0^\circ$  reads  $(\sin\phi_s)|_{\text{SM}} = -0.036 \pm 0.002$  [28].

As we have noted in Subsection 2.4, effective  $B_s^0$  decay lifetimes offer an interesting alternative for the extraction of  $\phi_s$  and  $\Delta\Gamma_s$ . This is also the case for the  $B_s^0 \rightarrow J/\psi f_0$  channel [74,75], where the situation corresponding to the current data is shown in Fig. 3. The  $B_s^0$  effective lifetime in the  $J/\psi f_0(980)$  final state is currently known with a precision of the order of 3% (see Section 2.4). The corresponding contour in the  $\phi_s$ – $\Delta\Gamma_s$  plane is very robust with respect to the hadronic penguin uncertainties, thereby nicely complementing the analysis of (63). A future measurement of the effective lifetime  $\tau_{J/\psi f_0}$  with 1% uncertainty would be most interesting.

A study of CP violation in the  $B_s^0 \rightarrow J/\psi f_0(980)$  decay was done by the LHCb collaboration [21], with the result

$$\phi_s = -0.44 \pm 0.44 \text{ (stat)} \pm 0.02 \text{ (syst)}. \quad (65)$$

In addition, LHCb studied  $B_s^0 \rightarrow J/\psi \pi^+ \pi^-$  decays [22], which includes both the  $f_0(980)$  and non-resonant final state. The obtained value of  $\phi_s$  is more precise

$$\phi_s = -0.019^{+0.173}_{-0.174} \text{ (stat)}^{+0.004}_{-0.003} \text{ (syst)}. \quad (66)$$

In view of the large errors in the value of  $\phi_s$ , the hadronic corrections discussed above are not yet relevant in this analysis. However, once the experimental result enters the SM range in (64), the hadronic phase shift  $\Delta\tilde{\phi}_s$  has to be controlled in order to match the theoretical and experimental precisions.

In order to obtain insights into these effects, it would be interesting to compare the separate measurements of  $\phi_s$  from  $B_s^0 \rightarrow J/\psi \phi$  and  $B_s^0 \rightarrow J/\psi f_0$  with each other as the hadronic penguin effects have a different impact on these determinations. With the LHCb upgrade project, the foreseen experimental uncertainties with  $50 \text{ fb}^{-1}$ , are equal to  $0.46^\circ$  and  $0.80^\circ$  for the  $B_s^0 \rightarrow J/\psi \phi$  and  $B_s^0 \rightarrow J/\psi f_0$  decays, respectively [76]. In particular, in the high-precision era of the LHCb upgrade, these measurements should not be averaged in a naive way, neglecting the hadronic corrections.

Another possibility to probe the penguin effects directly is offered by the  $B_d^0 \rightarrow J/\psi f_0$  channel. Estimates have shown that its branching ratio with  $f_0 \rightarrow \pi^+ \pi^-$  could be as large as  $\mathcal{O}(10^{-6})$  [28]. The translation of the corresponding penguin parameters into their counterparts entering the  $B_s \rightarrow J/\psi f_0$  mode depends unfortunately also on assumptions about the hadronic structure of the  $f_0(980)$ . However, a better picture of this still unsettled hadronic scalar state may be available once these challenging measurements can be performed in practice.

### 3.5 CP Violation in $B_s^0 \rightarrow J/\psi K_S$

The decay  $B_s^0 \rightarrow J/\psi K_S$  originates from  $\bar{b} \rightarrow \bar{c}c\bar{d}$  quark-level processes and is related to  $B_d^0 \rightarrow J/\psi K_S$  through the  $U$ -spin flavor symmetry of strong interactions, which relates down and strange quarks to each other in a manner similar to the  $SU(2)$  isospin symmetry connecting the up and down quarks [23]. In the SM, the decay amplitude of this channel can be written as

$$A(B_s^0 \rightarrow J/\psi K_S) = -\lambda \mathcal{A} (1 - ae^{i\theta} e^{i\gamma}), \quad (67)$$

which has a structure similar to (50). On the other hand, we have

$$A(B_d^0 \rightarrow J/\psi K_S) = (1 - \lambda^2/2) \mathcal{A}' (1 + \epsilon a' e^{i\theta'} e^{i\gamma}), \quad (68)$$

where the penguin parameter  $a' e^{i\theta'}$  enters in a doubly Cabibbo-suppressed way. The  $U$ -spin symmetry implies the relation

$$a' = a, \quad \theta' = \theta. \quad (69)$$

As was pointed out in Ref. [23], the information offered by the ratio of the  $B_{s,d} \rightarrow J/\psi K_S$  branching ratios and the direct and mixing-induced CP asymmetries of the  $B_s \rightarrow J/\psi K_S$  channel can be converted into the angle  $\gamma$  and the penguin parameters  $a$ ,  $\theta$  by means of the  $U$ -spin symmetry.

In 1999, the  $\gamma$  determination appeared the most interesting aspect of this strategy [23]. A feasibility study was performed in Ref. [27]. It showed that the extraction of  $\gamma$  looks feasible for the LHCb upgrade era but will probably not be competitive with other methods for the extraction of  $\gamma$ . On the other hand, if  $\gamma$  is used as an input, the penguin parameters  $a$  and  $\theta$  can be extracted in a theoretically clean way from the CP-violating  $B_s^0 \rightarrow J/\psi K_S$  asymmetries. Using (69), the penguin parameters affecting the extraction of the angle  $\beta$  of the unitarity triangle from the CP violation in  $B_d^0 \rightarrow J/\psi K_S$  can then be determined.

The extraction of  $a$  and  $\theta$  will be the key application of the  $B_s^0 \rightarrow J/\psi K_S$  channel. Since the dynamics is similar to that of the  $B_s^0 \rightarrow J/\psi \bar{K}^{*0}$ ,  $J/\psi \phi$  system, valuable insights into the size of the penguin uncertainties affecting the extraction of  $\phi_s$ , as discussed in Subsection 3.3, can be obtained.

The  $B_s \rightarrow J/\psi K_S$  channel has been observed by CDF [91] and LHCb [100], but so far only measurements of the branching ratio are available, where the subtleties related to the sizable  $B_s$  decay width difference  $\Delta\Gamma_s$  discussed in Subsection 2.3 have to be taken into account. A test of the  $SU(3)$  flavor symmetry is provided by the following relation [27, 100]:

$$\Xi_{SU(3)} \equiv \frac{\Phi_{J/\psi\pi^0}^d \tau_{B_d}}{\Phi_{J/\psi K_S}^s \tau_{B_s}} \left[ \frac{\text{BR}(B_s^0 \rightarrow J/\psi \bar{K}^{*0})_{\text{theo}}}{2\text{BR}(B_d^0 \rightarrow J/\psi \pi^0)_{\text{theo}}} \right] = 0.93 \pm 0.15, \quad (70)$$

where the  $\Phi$  and  $\tau_{B_q}$  denote phase-space factors and  $B_q$  lifetimes, respectively, and the ‘‘theoretical’’ branching ratios refer to the definition in (17). In this expression,

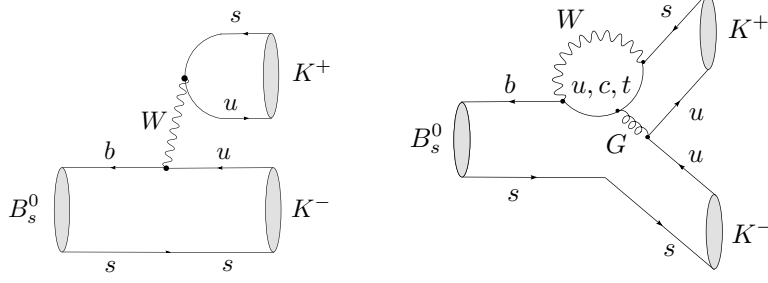


Figure 6: Illustration of the tree (left) and penguin (right) diagrams contributing to the  $B_s^0 \rightarrow K^+ K^-$  decay.

tiny penguin annihilation and exchange topologies (which can be constrained through experimental data) have been neglected. In the  $SU(3)$  limit, we have then  $\Xi_{SU(3)} = 1$ , which is consistent with the numerical value following from the current branching ratio measurement.

We look forward to future measurements of the effective  $B_s \rightarrow J/\psi K_S$  lifetime and the CP asymmetries of this channel.

### 3.6 CP Violation in $B_s^0 \rightarrow K^+ K^-$

The decay  $B_s^0 \rightarrow K^+ K^-$  originates from  $\bar{b} \rightarrow \bar{s}u\bar{u}$  quark-level transitions and receives contributions from tree and penguin topologies, as illustrated in Fig. 6. In the SM, the corresponding decay amplitude can be written as follows [101]:

$$A(B_s^0 \rightarrow K^+ K^-) = e^{i\gamma} \lambda \mathcal{C}' \left[ 1 + \frac{1}{\epsilon} d' e^{i\theta'} e^{-i\gamma} \right], \quad (71)$$

where  $\mathcal{C}'$  and  $d' e^{i\theta'}$  are CP-conserving parameters. While the former is governed by the tree topology, the latter is a measure of the ratio of the penguin to tree amplitudes. Interestingly, thanks to the peculiar CKM structure of (71), the  $B_s^0 \rightarrow K^+ K^-$  decay is dominated by the penguin topologies.

Looking at the diagrams in Fig. 6, we observe that we get the topologies for the  $B_d^0 \rightarrow \pi^+ \pi^-$  decay by interchanging the roles of all down and strange quarks. Consequently, the two decays are related to each other through the  $U$ -spin symmetry of strong interactions, in analogy to the  $B_{s,d} \rightarrow J/\psi K_S$  system discussed in Section 3.5. The corresponding decay amplitude is given in the SM as follows:

$$A(B_d^0 \rightarrow \pi^+ \pi^-) = e^{i\gamma} \left( 1 - \frac{\lambda^2}{2} \right) \mathcal{C} [1 - d e^{i\theta} e^{-i\gamma}], \quad (72)$$

where  $\mathcal{C}$  and  $d e^{i\theta}$  are the counterparts of the primed quantities in (71). The  $B_d^0 \rightarrow \pi^+ \pi^-$  channel is dominated by the tree contributions.

If we apply the  $U$ -spin symmetry, we obtain the relations [101]

$$d' = d, \quad \theta' = \theta. \quad (73)$$

As the  $B_{d,s}^0 - \bar{B}_{d,s}^0$  mixing phases are known, the direct and mixing-induced CP asymmetries of the  $B_d \rightarrow \pi^+ \pi^-$  and  $B_s \rightarrow K^+ K^-$  decays allow the determination of theoretically

clean contours in the  $\gamma$ - $d$  and  $\gamma$ - $d'$  planes, respectively. Using the first relation in (73),  $\gamma$  and the hadronic parameters  $d$ ,  $\theta$  and  $\theta'$  can be determined [101], where the strong phases  $\theta$  and  $\theta'$  offer an internal test of the  $U$ -spin symmetry.

In Refs. [102, 103], detailed discussions of this strategy can be found. The  $B_s^0 \rightarrow K^+K^-$  decay has been observed by the CDF [104], Belle [105] and LHCb [36] collaborations. Using the branching ratio information, non-perturbative QCD sum rule calculations of the form-factor ratio entering  $|\mathcal{C}'/\mathcal{C}|$  [107], and measurements of CP violation in  $B_d \rightarrow \pi^+\pi^-$ ,  $B_d \rightarrow \pi^\mp K^\pm$ , the following result for  $\gamma$  was determined in Ref. [103]:

$$\gamma = (68.3_{-5.7}^{+4.9}|_{\text{input}} +5.0|_{\xi}^{+0.1}|_{\Delta\theta}^{\circ})^\circ, \quad (74)$$

where the first error is due to the uncertainties of the input quantities, and the latter errors describe  $U$ -spin-breaking effects parametrized as  $\xi \equiv d'/d = 1 \pm 0.15$  and  $\Delta\theta \equiv \theta' - \theta = \pm 20^\circ$ . The result for  $\gamma$  in (74) is in excellent agreement with the fits of the unitarity triangle.

The usefulness of the effective  $B_s \rightarrow K^+K^-$  lifetime has already been addressed in Section 2.4 and Fig. 3. For a more detailed discussion, the reader is referred to Ref. [74].

A variant of the  $B_s \rightarrow K^+K^-$ ,  $B_d \rightarrow \pi^+\pi^-$  strategy for the extraction of  $\gamma$  discussed above has recently been discussed in [106]. The experimental prospects of the exploration of the  $B_s \rightarrow K^+K^-$ ,  $B_d \rightarrow \pi^+\pi^-$  system are promising for the LHCb experiment [76]. First results have been obtained by the LHCb collaboration using only a fraction of the 2011 data ( $0.69 \text{ fb}^{-1}$ ) [108]. In the notation of Eq. (25), these results read as follows:

$$\begin{aligned} C(B_s \rightarrow K^+K^-) &= -0.02 \pm 0.18(\text{stat}) \pm 0.04(\text{syst}) \stackrel{\text{SM}}{=} 0.098 \pm 0.04, \\ S(B_s \rightarrow K^+K^-) &= 0.17 \pm 0.18(\text{stat}) \pm 0.05(\text{syst}) \stackrel{\text{SM}}{=} 0.215_{-0.047}^{+0.060}, \end{aligned} \quad (75)$$

for comparison, we give also the SM predictions obtained in Ref. [103].

### 3.7 CP violation in $B_s^0 \rightarrow \pi^+K^-$

Another interesting decay is  $B_s^0 \rightarrow \pi^+K^-$ , which receives contributions from penguin and tree topologies and can be combined with  $B_d^0 \rightarrow \pi^-K^+$  to determine the CKM angle  $\gamma$  [102, 109, 110]. As this channel is flavor-specific, it does not exhibit mixing-induced CP violation. Using  $SU(3)$  flavor-symmetry arguments yields the relations

$$\begin{aligned} \mathcal{A}_{\text{CP}}^{\text{dir}}(B_s^0 \rightarrow \pi^+K^-) &\approx \mathcal{A}_{\text{CP}}^{\text{dir}}(B_d^0 \rightarrow \pi^+\pi^-) \\ &\approx - \left[ \frac{\text{BR}(B_d \rightarrow \pi^\mp K^\pm)}{\text{BR}(B_s \rightarrow \pi^\pm K^\mp)} \right] \mathcal{A}_{\text{CP}}^{\text{dir}}(B_d^0 \rightarrow \pi^-K^+) \end{aligned} \quad (76)$$

between the direct CP asymmetries of the  $B_s^0 \rightarrow \pi^+K^-$ ,  $B_d^0 \rightarrow \pi^-K^+$  and  $B_d^0 \rightarrow \pi^+\pi^-$  channels, arising from the interference between tree and penguin contributions. The  $B_d^0 \rightarrow \pi^-K^+$  decay has allowed the establishment of direct CP violation in the  $B$ -meson system [111–113], thereby complementing the measurement of direct CP violation in  $K_{L,S} \rightarrow \pi\pi$  decays through a non-vanishing value of the  $\text{Re}(\varepsilon'/\varepsilon)$  parameter by the KTeV [114] and NA48 [115] collaborations.

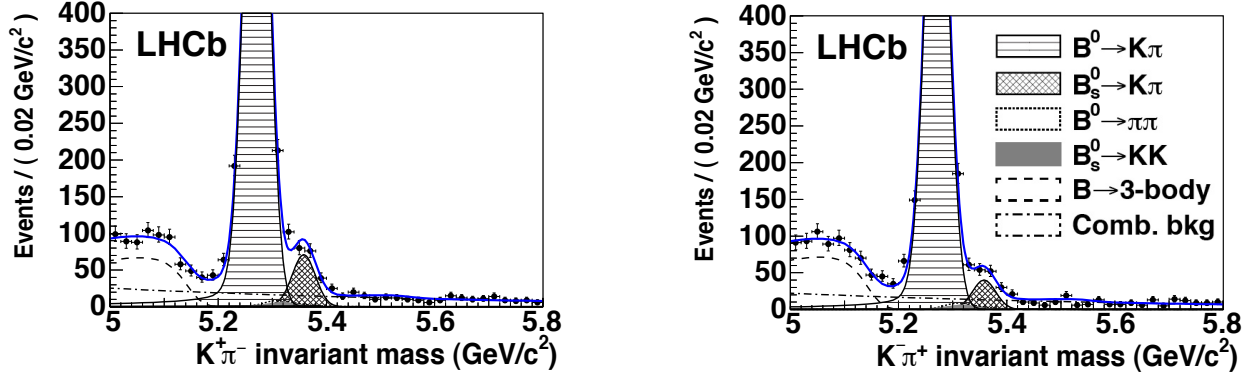


Figure 7: Invariant  $K\pi$  mass spectra. The right plot corresponds to the  $K^+\pi^-$  invariant mass while the left plot corresponds to the  $K^-\pi^+$  invariant mass. The results of the unbinned maximum likelihood fits are overlaid. The main components contributing to the fit model are also shown (from Ref. [117]).

The  $B_s^0 \rightarrow \pi^+ K^-$  channel has been extensively studied at the Tevatron [116] and the Belle experiment [112].

In 2012, the LHCb experiment has provided the first evidence of direct CP violation in this channel [117], confirmed later by the CDF experiment [118]:

$$\mathcal{A}_{\text{CP}}^{\text{dir}}(B_s^0 \rightarrow \pi^+ K^-) = 0.27 \pm 0.08 \text{ (stat)} \pm 0.02 \text{ (syst)} \text{ (LHCb)}, \quad (77)$$

$$\mathcal{A}_{\text{CP}}^{\text{dir}}(B_s^0 \rightarrow \pi^+ K^-) = 0.22 \pm 0.07 \text{ (stat)} \pm 0.02 \text{ (syst)} \text{ (CDF)}, \quad (78)$$

which is the first signal of CP violation in the  $B_s$ -meson system. The clear asymmetry is already visible from the raw signal yields from Fig. 7, and the result is consistent with the relations in (76) for the most recent measurements of CP violation in  $B_d^0 \rightarrow \pi^+ \pi^-$ .

### 3.8 CP Violation in $B_s \rightarrow D_s^\pm K^\mp$ Decays

In contrast to the modes discussed in the previous sections,  $B_s \rightarrow D_s^\pm K^\mp$  decays receive only contributions from tree-diagram-like topologies, i.e. there are no penguin contributions present. As can be seen in Fig. 8, both  $B_s^0$  and  $\bar{B}_s^0$  mesons can decay into the  $D_s^+ K^-$  final state. Consequently, interference effects between  $B_s^0$ - $\bar{B}_s^0$  mixing and decay processes lead to a time-dependent CP-violating rate asymmetry, which has the same form as the expression in (25). Moreover, both decay paths are of the same order  $\lambda^3$  in the Wolfenstein expansion [53], thereby leading to large interference effects. The corresponding CP asymmetries provide sufficient information to determine the phase  $\phi_s + \gamma$  in a theoretically clean way [119, 120]. The decay width difference  $\Delta\Gamma_s$  offers new observables for this method and allows an unambiguous determination of  $\phi_s + \gamma$  [120], as studied in Refs. [121]–[123]. For a detailed recent analysis of the  $B_s \rightarrow D_s^{(*)\pm} K^\mp$  system in view of the sizable  $\Delta\Gamma_s$ , the reader is referred to Ref. [124].

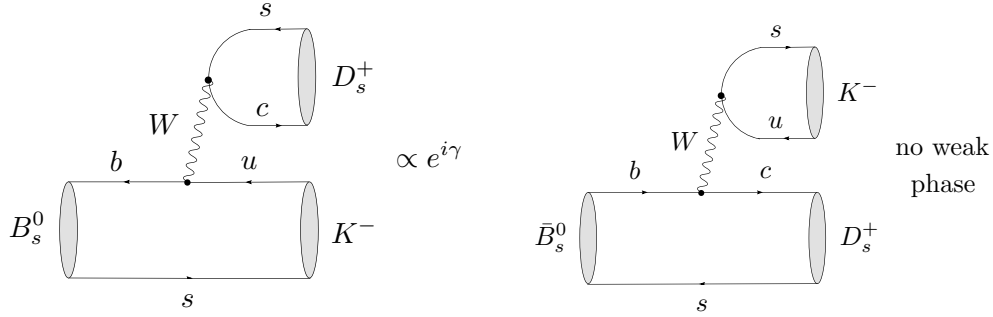


Figure 8: Feynman diagrams contributing to  $B_s^0 \rightarrow D_s^+ K^-$  and  $\bar{B}_s^0 \rightarrow D_s^+ K^-$  decays.

Concerning the experimental status, the CDF [125], Belle [126] and LHCb [127] collaborations have reported first measurements of the  $B_s \rightarrow D_s^\pm K^\mp$  branching ratio:

$$\frac{\text{BR}(B_s \rightarrow D_s^\pm K^\mp)_{\text{exp}}}{\text{BR}(B_s \rightarrow D_s^\pm \pi^\mp)_{\text{exp}}} = \begin{cases} 0.097 \pm 0.018 \text{ (stat.)} \pm 0.009 \text{ (syst.)} & [\text{CDF}], \\ 0.065_{-0.029}^{+0.035} \text{ (stat.)} & [\text{Belle}], \\ 0.0646 \pm 0.0043 \text{ (stat.)} \pm 0.0025 \text{ (syst.)} & [\text{LHCb}]; \end{cases} \quad (79)$$

the errors of the Belle result are dominated by the small  $B_s \rightarrow D_s^\pm K^\mp$  data sample. These branching ratios correspond to the “experimental” time-integrated branching ratios, as introduced in Eq. (16). In Ref. [124], it was pointed out that there is a theoretical lower bound of  $0.080 \pm 0.007$  for the ratio in (79). Using data for  $B_d \rightarrow D^\pm \pi^\mp$  decays and the  $SU(3)$  flavor symmetry results in a sharper picture, with the following prediction [124]:

$$\left. \frac{\text{BR}(B_s \rightarrow D_s^\pm K^\mp)_{\text{exp}}}{\text{BR}(B_s \rightarrow D_s^\pm \pi^\mp)_{\text{exp}}} \right|_{SU(3)} = 0.0864_{-0.0072}^{+0.0087}. \quad (80)$$

In addition to the ratio in (79), another interesting observable is provided by the following asymmetry (see also Ref. [128]):

$$\begin{aligned} & \frac{\text{BR}(B_s \rightarrow D_s^+ K^-)_{\text{exp}} - \text{BR}(B_s \rightarrow D_s^- K^+)_{\text{exp}}}{\text{BR}(B_s \rightarrow D_s^+ K^-)_{\text{exp}} + \text{BR}(B_s \rightarrow D_s^- K^+)_{\text{exp}}} \\ &= y_s \left[ \frac{\mathcal{A}_{\Delta\Gamma}(B_s \rightarrow D_s^+ K^-) - \mathcal{A}_{\Delta\Gamma}(B_s \rightarrow D_s^- K^+)}{2 + y_s \{\mathcal{A}_{\Delta\Gamma}(B_s \rightarrow D_s^+ K^-) + \mathcal{A}_{\Delta\Gamma}(B_s \rightarrow D_s^- K^+)\}} \right] \stackrel{SU(3)}{=} -0.027_{-0.019}^{+0.052}, \end{aligned} \quad (81)$$

where we give also the theoretical prediction following from the  $SU(3)$  flavor symmetry and the  $B_d \rightarrow D^\pm \pi^\mp$  data. An experimental non-vanishing value of (81) would establish a difference between the  $\mathcal{A}_{\Delta\Gamma}(B_s \rightarrow D_s^+ K^-)$  and  $\mathcal{A}_{\Delta\Gamma}(B_s \rightarrow D_s^- K^+)$  observables. The corresponding effective lifetimes defined in analogy to (19) offer also useful information [124, 128].

Using  $1 \text{ fb}^{-1}$  of  $pp$  collision data recorded in 2011 at a center of mass energy of  $\sqrt{s} = 7$  TeV, LHCb has reported the first measurement of the time-dependent CP asymmetries



of  $B_s^0 \rightarrow D_s^\mp K^\pm$  decays [129]. In the notation of Eq. (25), the results read as

$$\begin{aligned}
C(B_s \rightarrow D_s^+ K^-) &= -C(B_s \rightarrow D_s^- K^+) = -1.01 \pm 0.50(\text{stat}) \pm 0.23(\text{syst}), \\
S(B_s \rightarrow D_s^+ K^-) &= -1.25 \pm 0.56(\text{stat}) \pm 0.24(\text{syst}), \\
S(B_s \rightarrow D_s^- K^+) &= -0.08 \pm 0.68(\text{stat}) \pm 0.28(\text{syst}), \\
\mathcal{A}_{\Delta\Gamma}(B_s \rightarrow D_s^+ K^-) &= -1.33 \pm 0.60(\text{stat}) \pm 0.26(\text{syst}), \\
\mathcal{A}_{\Delta\Gamma}(B_s \rightarrow D_s^- K^+) &= -0.81 \pm 0.56(\text{stat}) \pm 0.26(\text{syst}). \quad (82)
\end{aligned}$$

Since  $\phi_s$  is known from analyses of the  $B_s \rightarrow J/\psi\phi$  and  $B_s \rightarrow J/\psi f_0$  decays as we have discussed in Subsections 3.3 and 3.4, the phase  $\phi_s + \gamma$  which can be extracted in the future from these measurements can be straightforwardly converted into  $\gamma$ . This determination complements nicely the well-established time-integrated methods to extract  $\gamma$  from  $B^- \rightarrow D^{(*)}K^{(*)-}$  and  $B_d^0 \rightarrow D^0 K^{*0}$ , which are also pure tree-level decays [76].

### 3.9 Further $B_s$ Decays to Explore CP Violation

The  $B_s$ -meson system offers various other decays with an interesting physics potential for the exploration of CP violation. Since a detailed presentation goes beyond the scope of this review, let us just briefly list promising channels.

The decay  $B_s^0 \rightarrow D_s^+ D_s^-$  originates from  $\bar{b} \rightarrow \bar{c}c\bar{s}$  quark-level processes, and receives contributions from a tree topology and doubly Cabibbo-suppressed penguin amplitudes. It offers yet another determination of the  $B_s^0$ - $\bar{B}_s^0$  mixing phase  $\phi_s$  and can be combined with the  $B_d^0 \rightarrow D_d^+ D_d^-$  channel through the  $U$ -spin symmetry to extract the CKM angle  $\gamma$  and the relevant penguin parameters [23, 130]. Performing an angular analysis, information about  $\phi_s$  can also be extracted from the  $B_s^0 \rightarrow D_s^{*+} D_s^{*-}$  channel. A first step towards this analysis is the measurement of the branching fraction of the  $B_s^0 \rightarrow D_s^+ D_s^-$  decay mode. It has been measured relative to the  $B_d^0 \rightarrow D_s^+ D^-$  channel by the LHCb collaboration with  $1 \text{ fb}^{-1}$  [131]:

$$\frac{\text{BR}(B_s^0 \rightarrow D_s^+ D_s^-)}{\text{BR}(B_d^0 \rightarrow D_s^+ D^-)} = 0.508 \pm 0.026(\text{stat}) \pm 0.043(\text{syst}) \quad (83)$$

in good agreement with the current world average [68] but with an higher precision.

The  $B_s^0 \rightarrow K^{*0} \bar{K}^{*0}$  mode is caused by  $\bar{b} \rightarrow \bar{d}d\bar{s}$  transitions and receives therefore only contributions from penguin topologies. It is hence of interesting to test the SM description of CP violation. The  $B_s^0 \rightarrow K^{*0} \bar{K}^{*0}$  decay can be related to the  $B_d^0 \rightarrow K^{*0} \bar{K}^{*0}$  channel by means of the  $U$ -spin symmetry, thereby allowing the extraction of  $\phi_s$  and  $\gamma$  from the observables of the time-dependent angular distribution [132]. The  $B_s^0 \rightarrow K^{*0} \bar{K}^{*0}$  mode has received increasing interest in the context with the determination of  $\phi_s$  [73, 133–135], and the LHCb collaboration has recently reported the first observation of this channel [72].

The final  $B_s$  decay of our discussion of CP violation is the  $B_s^0 \rightarrow \phi\phi$  channel, which is caused by  $\bar{b} \rightarrow \bar{s}s\bar{s}$  quark-level processes. It is again a pure penguin decay, which offers a sensitive probe to new sources of CP violation; for a detailed recent theoretical

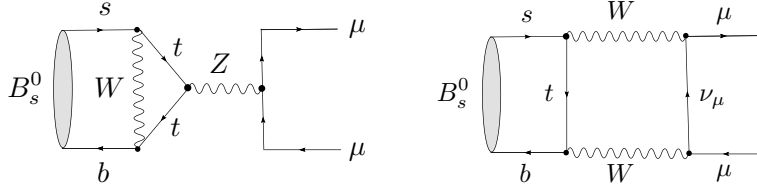


Figure 9: Decay topologies contributing to the  $B_s^0 \rightarrow \mu^+ \mu^-$  decay in the SM.

analysis see Ref. [136]. It will be exciting to measure its time-dependent CP-violating rate asymmetry at the LHCb experiment. So far, only time-integrated measurements of angular distributions are available [137, 138]. Such measurements offer interesting analyses of triple product asymmetries [139, 140].

## 4 Rare Decays of $B_s^0$ Mesons

### 4.1 The $B_s^0 \rightarrow \mu^+ \mu^-$ Decay

In the SM, the rare decay  $B_s \rightarrow \mu^+ \mu^-$  originates from loop contributions, as illustrated in Fig. 9. Moreover, as only leptons are present in the final state, the hadronic sector is simply described by the non-perturbative  $B_s$  decay constant  $f_{B_s}$ . The  $B_s \rightarrow \mu^+ \mu^-$  channel is one of the cleanest rare  $B$  decays and therefore offers a powerful probe to search for NP effects which may enter through new particles running in the loops or even through new flavor-changing neutral current contributions at the tree level (see [83] and references therein).

The most recent theoretical update of the  $B_s \rightarrow \mu^+ \mu^-$  branching ratio arising in the SM is given as follows [141]:

$$\text{BR}(B_s \rightarrow \mu^+ \mu^-)_{\text{SM}} = (3.23 \pm 0.27) \times 10^{-9}, \quad (84)$$

where the error is dominated by the lattice QCD value of  $B_s$  decay constant  $f_{B_s}$ . The extremely small branching ratio makes the experimental search and analysis of this rare decay very challenging.

For the following discussion, it is useful to have a closer look at the theoretical description of the  $\bar{B}_s^0 \rightarrow \mu^+ \mu^-$  channel. The starting point is an appropriate low-energy effective Hamiltonian [142]. Using the same notation as in [143], it can be written as follows:

$$\mathcal{H}_{\text{eff}} = -\frac{G_F}{\sqrt{2}\pi} \alpha V_{ts}^* V_{tb} [C_{10} O_{10} + C_S O_S + C_P O_P + C'_{10} O'_{10} + C'_S O'_S + C'_P O'_P]. \quad (85)$$

Here  $G_F$  and  $\alpha$  are the Fermi and QED fine-structure constants, respectively, and the  $V_{qq'}$  are CKM matrix elements. The short-distance physics is encoded in the Wilson coefficients  $C_i$ ,  $C'_i$  of the four-fermion operators

$$O_{10} = (\bar{s} \gamma_\mu P_L b) (\bar{\ell} \gamma^\mu \gamma_5 \ell), \quad O_S = m_b (\bar{s} P_R b) (\bar{\ell} \ell), \quad O_P = m_b (\bar{s} P_R b) (\bar{\ell} \gamma_5 \ell), \quad (86)$$

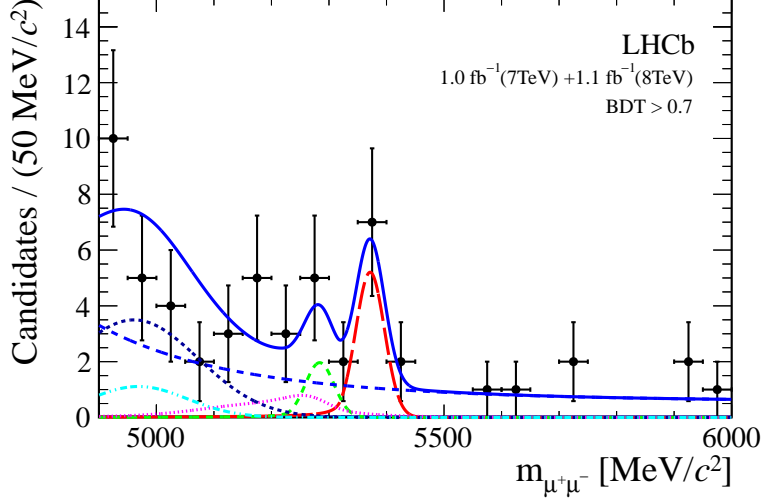


Figure 10: Invariant mass distribution of the selected  $B_s^0 \rightarrow \mu^+\mu^-$  candidates (black dots) in a signal enriched region [35]. The result of the fit is overlaid (blue solid line) and the different component detailed:  $B_s^0 \rightarrow \mu^+\mu^-$  (red long dashed),  $B_d^0 \rightarrow \mu^+\mu^-$  (green medium dashed),  $B_{(s)}^0 \rightarrow h^+h'^-$  (pink dotted),  $B_d^0 \rightarrow \pi^-\mu^+\nu_\mu$  (black short dashed) and  $B^{0(+)} \rightarrow \pi^{0(+)}\mu^+\mu^-$  (light blue dot dashed), and the combinatorial background (blue medium dashed).

where  $P_{L,R} \equiv (1 \mp \gamma_5)/2$ ,  $m_b$  is the  $b$ -quark mass, and the  $O'_i$  are obtained from the  $O_i$  through the replacements  $P_L \leftrightarrow P_R$ . All matrix elements can be expressed in terms of the  $B_s$ -meson decay constant  $f_{B_s}$ .

In the SM, (85) simplifies considerably. Then we have to deal only with  $O_{10}$  and its real Wilson coefficient  $C_{10}^{\text{SM}}$ , which governs the SM prediction in (84). Concerning the search for NP effects, the  $\bar{B}_s^0 \rightarrow \mu^+\mu^-$  decay has the outstanding feature to offer sensitivity to the (pseudo)-scalar lepton densities entering the  $O_{(P)S}$  and  $O'_{(P)S}$  operators, which is particularly relevant for models with extended Higgs sectors. The Wilson coefficients of these operators are still largely unconstrained by the current data (see, for instance, [143]).

The first step for the experimental exploration of the  $B_s \rightarrow \mu^+\mu^-$  decay is the measurement of the branching ratio. Since it is experimentally very challenging to measure the muon helicity, we consider the untagged combination

$$\langle \Gamma(B_s(t) \rightarrow \mu^+\mu^-) \rangle \equiv \sum_{\lambda=L,R} [\Gamma(B_s^0(t) \rightarrow \mu_\lambda^+\mu_\lambda^-) + \Gamma(\bar{B}_s^0(t) \rightarrow \mu^+\mu^-)]. \quad (87)$$

Ignoring the time information in this rate, we obtain the time-integrated “experimental branching” ratio as defined in Eq. (16).

The search for  $B_s \rightarrow \mu^+\mu^-$  at the Tevatron experiments has finally reached the region of about ten times the SM value (84), where DØ and CDF obtain the upper bounds  $5.1 \times 10^{-8}$  [31] and  $4.0 \times 10^{-8}$  [32] for the branching ratio at 95 % C.L., respectively. The search has been continued by the LHC experiments [33, 34, 144], reaching a combined

limit of  $\text{BR}(B_s^0 \rightarrow \mu^+ \mu^-) < 4.2 \cdot 10^{-9}$  (95 % C.L.), which is only 20% larger than the SM prediction.

In November 2012, the LHCb collaboration has reported the first evidence for  $B_s^0 \rightarrow \mu^+ \mu^-$  at the  $3.5\sigma$  level, with the following branching ratio [35]:

$$\text{BR}(B_s \rightarrow \mu^+ \mu^-) = (3.2_{-1.2}^{+1.5}) \times 10^{-9}. \quad (88)$$

The invariant mass distribution of the  $B_s^0 \rightarrow \mu^+ \mu^-$  candidates in a signal enriched region is shown in Fig. 10.

While the experimental upper bounds and the LHCb result in (88) refer to (87) and the time-integrated “experimental” branching ratio (16), the SM prediction in Eq. (88) refers to the “theoretical” branching ratio defined in (17). As was pointed out in Ref. [41], the conversion between these two branching ratio concepts is given by the following expression:

$$\text{BR}(B_s \rightarrow \mu^+ \mu^-)_{\text{theo}} = \left[ \frac{1 - y_s^2}{1 + \mathcal{A}_{\Delta\Gamma} y_s} \right] \text{BR}(B_s \rightarrow \mu^+ \mu^-)_{\text{exp}}, \quad (89)$$

where it is essential that the observable

$$\mathcal{A}_{\Delta\Gamma} = \frac{|P|^2 \cos 2\varphi_P - |S|^2 \cos 2\varphi_S}{|P|^2 + |S|^2} \quad (90)$$

does not depend on the muon helicity (note also that  $f_{B_s}$  cancels). Here the combinations of Wilson coefficients

$$P \equiv |P| e^{i\varphi_P} \equiv \frac{C_{10} - C'_{10}}{C_{10}^{\text{SM}}} + \frac{M_{B_s}^2}{2m_\mu} \left( \frac{m_b}{m_b + m_s} \right) \left( \frac{C_P - C'_P}{C_{10}^{\text{SM}}} \right) \quad (91)$$

and

$$S \equiv |S| e^{i\varphi_S} \equiv \sqrt{1 - 4 \frac{m_\mu^2}{M_{B_s}^2} \frac{M_{B_s}^2}{2m_\mu} \left( \frac{m_b}{m_b + m_s} \right) \left( \frac{C_S - C'_S}{C_{10}^{\text{SM}}} \right)} \quad (92)$$

with their CP-violating phases  $\varphi_{P,S}$  have been introduced in such a way that  $P = 1$  and  $S = 0$  in the SM. In (90), the NP contribution to the  $B_s^0 - \bar{B}_s^0$  mixing phase (5) was neglected. This effect can straightforwardly be included through  $2\varphi_{P,S} \rightarrow 2\varphi_{P,S} - \phi_s^{\text{NP}}$ . However, the LHCb data for CP violation in  $B_s \rightarrow J/\psi\phi, J/\psi f_0(980)$  already constrain  $\phi_s^{\text{NP}}$  to the few-degree level (see Subsections 3.3 and 3.4), whereas the  $\varphi_{P,S}$  are still essentially unconstrained.

As can be seen in (90), since NP may enter through the Wilson coefficients, the  $\mathcal{A}_{\Delta\Gamma}$  observable is currently unknown. On the other hand, the SM gives the theoretically clean prediction of  $\mathcal{A}_{\Delta\Gamma}^{\text{SM}} = +1$ . Using (89), we hence rescale the theoretical SM branching ratio in (84) by a factor of  $1/(1 - y_s)$ , yielding

$$\text{BR}(B_s \rightarrow \mu^+ \mu^-)_{\text{SM}}|_{y_s} = (3.54 \pm 0.30) \times 10^{-9} \quad (93)$$

for the value of  $y_s$  in (14). This is the SM reference value for the comparison with the experimental branching ratio (88).

Once the currently emerging  $B_s \rightarrow \mu^+ \mu^-$  signal has been well established and more data become available, also the decay-time information for the untagged data sample can be included, which will allow the measurement of the effective lifetime  $B_s \rightarrow \mu^+ \mu^-$  lifetime, which is defined in analogy to (19) [40,41]. The effective lifetime allows the conversion of the experimental  $B_s \rightarrow \mu^+ \mu^-$  branching ratio into its theoretical counterpart through an expression that is analogous to (20). Moreover, also the observable

$$\mathcal{A}_{\Delta\Gamma} = \frac{1}{y_s} \left[ \frac{(1 - y_s^2)\tau_{\mu^+\mu^-} - (1 + y_s^2)\tau_{B_s}}{2\tau_{B_s} - (1 - y_s^2)\tau_{\mu^+\mu^-}} \right] \quad (94)$$

can be extracted from the data.

These measurements offer exciting new aspects for the exploration of the  $B_s \rightarrow \mu^+ \mu^-$  decay at the high-luminosity upgrade of the LHC. An extrapolation from current measurements of the effective  $B_s \rightarrow J/\psi f_0(980)$  and  $B_s \rightarrow K^+ K^-$  lifetimes by the CDF and LHCb collaborations to  $\tau_{\mu^+\mu^-}$  indicates that a precision of 5% or better may be feasible [41]. Detailed experimental studies are strongly encouraged.

The  $\Delta\Gamma_s$  effects propagate also into the NP constraints that can be obtained from the comparison of the experimental  $B_s \rightarrow \mu^+ \mu^-$  branching ratio with the SM, where it is useful to introduce the following ratio [41]:

$$R \equiv \frac{\text{BR}(B_s \rightarrow \mu^+ \mu^-)_{\text{exp}}}{\text{BR}(B_s \rightarrow \mu^+ \mu^-)_{\text{SM}}} = \left[ \frac{1 + y_s \cos 2\varphi_P}{1 - y_s^2} \right] |P|^2 + \left[ \frac{1 - y_s \cos 2\varphi_S}{1 - y_s^2} \right] |S|^2. \quad (95)$$

Using (84) and (88) yields  $R = 1.0_{-0.4}^{+0.5}$ , where the errors have been added in quadrature.

The  $R$  ratio can be converted into ellipses in the  $|P|-|S|$  plane which depend on the CP-violating phases  $\varphi_{P,S}$ . Since the latter quantities are unknown,  $R$  fixes actually a circular band with the upper bounds  $|P|, |S| \leq \sqrt{(1 + y_s)R}$ . As the experimental information on  $R$  does not allow us to separate the  $S$  and  $P$  contributions, still significant NP contributions may be hiding in the  $B_s \rightarrow \mu^+ \mu^-$  channel.

This situation can be resolved by measuring the effective lifetime  $\tau_{\mu^+\mu^-}$  and the associated  $\mathcal{A}_{\Delta\Gamma}$  observable, as illustrated in the figures shown in [41].

In the most recent analyses of the constraints on NP parameter space that are implied by the experimental upper bound on the  $B_s \rightarrow \mu^+ \mu^-$  branching ratio for various extensions of the SM, authors have now started to take the effect of  $\Delta\Gamma_s$  into account (see, for instance, [145]–[147] and the papers in [148]–[156]).

## 4.2 The $B_s^0 \rightarrow \phi\gamma$ Decay

Another interesting rare  $B_s^0$  decay is the  $B_s^0 \rightarrow \phi\gamma$  channel, which arises in the SM from penguin topologies. It is the  $B_s$  counterpart of the  $B_d^0 \rightarrow K^{*0}\gamma$  mode and originates from  $\bar{b} \rightarrow \bar{s}\gamma$  quark-level processes. The data for  $B_d^0 \rightarrow K^{*0}\gamma$  and the inclusive  $B \rightarrow X_s\gamma$  mode are in agreement with the SM within the errors and have put strong constraints on NP models.

The SM prediction reads  $\text{BR}(B_s^0 \rightarrow \phi\gamma) = (4.3 \pm 1.4) \times 10^{-5}$  [157], where the uncertainty is due to the non-perturbative QCD effects which are encoded in the corresponding form factors. A more precise theoretical prediction is given for the ratio  $\text{BR}(B_d^0 \rightarrow K^{*0}\gamma)/\text{BR}(B_s^0 \rightarrow \phi\gamma) = 1.0 \pm 0.2$  [157].

The decay  $B_s^0 \rightarrow \phi\gamma$  was first measured by the Belle collaboration [158]:

$$\text{BR}(B_s^0 \rightarrow \phi\gamma) = [5.7_{-1.5}^{+1.8}(\text{stat})_{-1.1}^{+1.2}(\text{syst})] \times 10^{-5}. \quad (96)$$

Recently, the LHCb collaboration published [159] the measurement of the ratio

$$\frac{\text{BR}(B_d^0 \rightarrow K^{*0}\gamma)}{\text{BR}(B_s^0 \rightarrow \phi\gamma)} = 1.12 \pm 0.08(\text{stat})_{-0.04}^{+0.06}(\text{syst})_{-0.08}^{+0.09}(\text{frag}). \quad (97)$$

The last uncertainty is due to the ratio  $f_s/f_d$  of fragmentation fractions discussed in Subsection 1.3. This result was obtained using  $0.37 \text{ fb}^{-1}$  of  $pp$  collisions at LHC. Using this measurement and the world average value [68] of the  $\text{BR}(B_d^0 \rightarrow K^{*0}\gamma)$ , the LHCb collaboration has obtained the currently most precise measurement of  $\text{BR}(B_s^0 \rightarrow \phi\gamma)$ , which is given by

$$\text{BR}(B_s^0 \rightarrow \phi\gamma) = (3.9 \pm 0.5) \times 10^{-5}. \quad (98)$$

The obtained experimental results are consistent with each other and with the SM prediction.

An interesting aspect of the  $B_s^0 \rightarrow \phi\gamma$  channel is that  $\Delta\Gamma_s$  offers an observable, which allows to measure the photon polarization and is sensitive to right-handed currents appearing in scenarios of physics beyond the SM [160]. This feature distinguishes  $B_s^0 \rightarrow \phi\gamma$  from  $B_d^0 \rightarrow K^{*0}\gamma$  as  $\Delta\Gamma_d$  is negligibly small.

### 4.3 The $B_s^0 \rightarrow \phi\mu^+\mu^-$ Decay

Another interesting rare decay is  $B_s^0 \rightarrow \phi\mu^+\mu^-$ , which is the  $B_s$  counterpart of the well-known  $B_d^0 \rightarrow K^{*0}\mu^+\mu^-$  channel. For a detailed study of the theoretical aspects of the  $B_s^0 \rightarrow \phi\mu^+\mu^-$  mode, we refer the reader to Ref. [161].

The CDF collaboration performed an extensive study of decays originating from  $b \rightarrow s\mu^+\mu^-$  quark-level processes with different hadrons in the initial and final states. The analysis is based on the statistics corresponding to  $9.6 \text{ fb}^{-1}$  of  $p\bar{p}$  collisions. This result [162] was still unpublished at the time of preparing this review. In each case the branching fraction of the decay  $H_b \rightarrow h\mu^+\mu^-$  is normalized to the well identified decay  $H_b \rightarrow J/\psi h$  with  $J/\psi \rightarrow \mu^+\mu^-$ . Such a normalization significantly reduces the systematic uncertainty of the measurements. The following result for the decay  $B_s^0 \rightarrow \phi\mu^+\mu^-$  is obtained:

$$\text{Br}(B_s^0 \rightarrow \phi\mu^+\mu^-) = [1.17 \pm 0.18(\text{stat}) \pm 0.37(\text{syst})] \times 10^{-6}. \quad (99)$$

These measurements are continued by the LHCb experiment which has recently obtained with  $1 \text{ fb}^{-1}$  [163]:

$$\text{Br}(B_s^0 \rightarrow \phi\mu^+\mu^-) = [0.78 \pm 0.10(\text{stat}) \pm 0.06(\text{syst}) \pm 0.28(\text{BR})] \times 10^{-6} \quad (100)$$

where the last uncertainty comes from the knowledge of the  $B_s^0 \rightarrow J/\psi\phi$  branching fraction. In future, a better precision, could reveal possible NP contributions. In particular angular analyses, similar to those performed for the  $B_d^0 \rightarrow K^{*0}\mu^+\mu^-$  decay, will be extremely interesting.

## 5 Conclusions and Outlook

The  $B_s$ -meson system plays a key role in the testing of the quark-flavor sector of the SM. After pioneering work at the Tevatron and measurements at the Belle experiment, the exploration of weak decays of  $B_s$  mesons has now fully shifted to the LHC. In 2012, we have seen two particularly exciting developments in the exploration of the  $B_s$  system: the common efforts of the Tevatron and LHC experiments has established a non-vanishing decay width difference  $\Delta\Gamma_s$ , and the first evidence for the rare decay  $B_s^0 \rightarrow \mu^+\mu^-$  has been reported at the  $3.5\sigma$  level by the LHCb experiment, thereby complementing the previous constraints from the CDF, DØ ATLAS and CMS collaborations. Both measurements are in accordance with the SM although the branching ratio of  $B_s^0 \rightarrow \mu^+\mu^-$  has still a large error. It will be very interesting to monitor the future evolution of the experimental picture.

Concerning the theoretical aspects of these results, the sizable value of  $\Delta\Gamma_s$  leads to subtleties in the interpretation of time-integrated  $B_s$  rates in terms of branching ratios but provides also new observables which can be accessed through effective  $B_s$  decay lifetimes. The emerging signal for the  $B_s^0 \rightarrow \mu^+\mu^-$  decay has entered many analyses of specific NP models, in particular supersymmetric scenarios, where strong constraints on the corresponding parameter space emerge. The effective lifetime of  $B_s \rightarrow \mu^+\mu^-$  offers a new, theoretically clean observable for the search for NP that is complementary to the branching ratio. Detailed studies for the high-luminosity upgrade of the LHC are strongly encouraged.

In the exploration of CP violation in the  $B_s$ -meson system, we have seen more precise experimental analyses of the benchmark decays  $B_s^0 \rightarrow J/\psi\phi$  and  $B_s^0 \rightarrow J/\psi f_0$  in 2012. The resulting picture of smallish CP violation – with  $\phi_s$  in the few degree regime – is again consistent with the SM description of CP violation through the Kobayashi–Maskawa mechanism. In view of this development, penguin contributions to the corresponding decay amplitudes have to be controlled. Since these topologies enter in a doubly Cabibbo-suppressed way they are usually neglected. However, once the experimental precision increases further, in particular at the LHCb upgrade, these effects may lead to fake NP signals and it will be crucial to match the experimental with the theoretical precision. Thanks to their non-perturbative nature, experimental control channels have to be used to probe the importance of the penguin contributions. In this context, the  $B_s^0 \rightarrow J/\psi K_S$  and  $B_s^0 \rightarrow J/\psi \bar{K}^{*0}$  decays play key roles, where first measurements of branching ratios and angular observables are already available. Another highlight of the exploration of CP violation is the  $B_s^0 \rightarrow \pi^+K^-$  channel, where LHCb and CDF established a direct CP asymmetry in 2012, which is again in accordance with the SM and  $SU(3)$  relations to the direct CP asymmetries of the  $B_d^0 \rightarrow \pi^-K^+$  and  $B_d^0 \rightarrow \pi^+\pi^-$  modes. Important first steps in the measurement of CP violation in the  $B_s \rightarrow K^+K^-$  and  $B_s \rightarrow D_s^\pm K^\mp$  channels could also be made by LHCb.

We look forward to many more exciting results in the exploration of rare decays and CP violation in the  $B_s$  system!

## References

- [1] D. Decamps *et al.* [ALEPH Collaboration], *Nucl. Instrum. Methods in Phys. Res. A* **294**, 121 (1990).
- [2] P. Aarnio *et al.* [DELPHI Collaboration], *Nucl. Instrum. Methods in Phys. Res. A* **303**, 233 (1991).
- [3] K. Ahmet *et al.* [OPAL Collaboration], *Nucl. Instrum. Methods in Phys. Res. A* **305**, 275 (1991).
- [4] A. Abulencia *et al.* [CDF Collaboration], *J. Phys. G* **34**, 2457 (2007).  
A. Sill *et al.*, *Nucl. Instrum. Methods in Phys. Res. A* **447**, 1 (2000). A. Affolder *et al.* [CDF Collaboration], *Nucl. Instrum. Methods in Phys. Res. A* **526**, 249 (2004).  
C. S. Hill [on behalf of the CDF Collaboration], *Nucl. Instrum. Methods in Phys. Res. A* **530**, 1 (2004).
- [5] G. Ascoli *et al.*, *Nucl. Instrum. Methods in Phys. Res. A* **268**, 33 (1988).  
T. Dorigo *et al.*, *Nucl. Instrum. Methods in Phys. Res. A* **461**, 560 (2001).
- [6] E. J. Thomson *et al.*, *IEEE Trans. Nucl. Sci.* **49**, 1063 (2002). J. A. Adelman *et al.* [CDF Collaboration], *Nucl. Instrum. Methods in Phys. Res. A* **572**, 361 (2007).  
A. Abulencia *et al.* [CDF Collaboration], *Phys. Rev. Lett.* **98**, 122002 (2007).
- [7] V.M. Abazov *et al.* [D0 Collaboration], *Nucl. Instrum. Methods in Phys. Res. A* **565**, 463 (2006).  
S.N. Ahmed *et al.*, *Nucl. Instrum. Methods in Phys. Res. A* **634**, 8 (2011);  
R. Angstadt *et al.*, *Nucl. Instrum. Methods in Phys. Res. A* **622**, 298 (2010).
- [8] V.M. Abazov *et al.*, *Nucl. Instrum. Methods in Phys. Res. A* **552**, 372 (2005).
- [9] A.A. Alves Jr. *et al.* [LHCb collaboration], *JINST* **3** (2008) S08005.
- [10] N. Cabibbo, *Phys. Rev. Lett.* **10**, 531 (1963).
- [11] M. Kobayashi and T. Maskawa, *Prog. Theor. Phys.* **49**, 652 (1973).
- [12] A. J. Buras and J. Girrbach, *Acta Phys. Polon. B* **43**, 1427 (2012) [arXiv:1204.5064 [hep-ph]].
- [13] V. Abazov *et al.* [D0 Collaboration], *Phys. Rev. D* **84**, 052007 (2011).
- [14] V. Abazov *et al.* [D0 Collaboration], *Phys. Rev. D* **86**, 072009 (2012).
- [15] V. Abazov *et al.* [D0 Collaboration], arXiv:1207.1769 [hep-ex] (2012).
- [16] LHCb collaboration, Conference report LHCb-CONF-2012-022 (2012).
- [17] T. Aaltonen *et al.* [CDF Collaboration], *Phys. Rev. Lett.* **109**, 171802 (2012).
- [18] V.M. Abazov *et al.* [D0 Collaboration], *Phys. Rev. D* **85**, 032006 (2012).



- [19] R. Aaij *et al.* [LHCb Collaboration], *Phys. Rev. Lett.* **108**, 101803 (2012).
- [20] G. Aad *et al.* [ATLAS Collaboration], arXiv: 1208.0572 [hep-ex] (2012).
- [21] R. Aaij *et al.* [LHCb Collaboration], *Phys. Lett. B* **707**, 497 (2012).
- [22] R. Aaij *et al.* [LHCb Collaboration], *Phys. Lett. B* **713**, 378 (2012).
- [23] R. Fleischer, *Eur. Phys. J. C* **10**, 299 (1999) [hep-ph/9903455].
- [24] M. Ciuchini, M. Pierini and L. Silvestrini, *Phys. Rev. Lett.* **95**, 221804 (2005) [hep-ph/0507290]; arXiv:1102.0392 [hep-ph].
- [25] S. Faller, R. Fleischer, M. Jung and T. Mannel, *Phys. Rev. D* **79**, 014030 (2009) [arXiv:0809.0842 [hep-ph]].
- [26] S. Faller, R. Fleischer and T. Mannel, *Phys. Rev. D* **79**, 014005 (2009) [arXiv:0810.4248 [hep-ph]].
- [27] K. De Bruyn, R. Fleischer and P. Koppenburg, *Eur. Phys. J. C* **70**, 1025 (2010) [arXiv:1010.0089 [hep-ph]].
- [28] R. Fleischer, R. Knegjens and G. Ricciardi, *Eur. Phys. J. C* **71**, 1832 (2011) [arXiv:1109.1112 [hep-ph]].
- [29] R. Fleischer, R. Knegjens and G. Ricciardi, *Eur. Phys. J. C* **71**, 1798 (2011) [arXiv:1110.5490 [hep-ph]].
- [30] M. Jung, *Phys. Rev. D* **86**, 053008 (2012) [arXiv:1206.2050 [hep-ph]].
- [31] V. M. Abazov *et al.* [D0 Collaboration], *Phys. Lett. B* **693**, 539 (2010) [arXiv:1006.3469].
- [32] T. Aaltonen *et al.* [CDF Collaboration], *Phys. Rev. Lett.* **107**, 191801 (2011) [arXiv:1107.2304].
- [33] S. Chatrchyan *et al.* [CMS Collaboration], *JHEP* **04**, 033 (2012) [arXiv:1203.3976].
- [34] G. Aad *et al.* [ATLAS Collaboration], *Phys. Lett. B* **713**, 387 (2012) [arXiv:1204.0735].
- [35] R. Aaij *et al.* [LHCb Collaboration], *Phys. Rev. Lett.* **110**, 021801 (2013).
- [36] R. Aaij *et al.* [LHCb Collaboration], *Phys. Lett. B* **707**, 349 (2012).
- [37] R. Aaij *et al.* [LHCb Collaboration], *Phys. Lett. B* **716**, 393 (2012).
- [38] T. Aaltonen *et al.* [CDF Collaboration], *Phys. Rev. D* **84**, 052012 (2011).
- [39] R. Aaij *et al.* [LHCb Collaboration], *Phys. Rev. Lett.* **109**, 152002 (2012).

- [40] K. De Bruyn, R. Fleischer, R. Knegjens, P. Koppenburg, M. Merk and N. Tuning, *Phys. Rev. D* **86**, 014027 (2012) [arXiv:1204.1735 [hep-ph]].
- [41] K. De Bruyn, R. Fleischer, R. Knegjens, P. Koppenburg, M. Merk, A. Pellegrino and N. Tuning, *Phys. Rev. Lett.* **109**, 041801 (2012) [arXiv:1204.1737 [hep-ph]].
- [42] R. Aaij *et al.* [LHCb Collaboration], arXiv:1211.3055, submitted to JINST.
- [43] ATLAS Collaboration, JINST, 3:S08003, 2008.
- [44] CMS Collaboration, JINST, 3:S08004, 2008.
- [45] T. Sjostrand, S. Mrenna, and P. Skands, *JHEP* **05**, 026 (2006) [arXiv:hep-ph/0603175].
- [46] R. Aaij *et al.*, *Eur. Phys. J. C* **71**, 1645 (2011).
- [47] R. Fleischer, N. Serra and N. Tuning, *Phys. Rev. D* **82**, 034038 (2010) [arXiv:1004.3982 [hep-ph]].
- [48] R. Fleischer, N. Serra and N. Tuning, *Phys. Rev. D* **83**, 014017 (2011) [arXiv:1012.2784 [hep-ph]].
- [49] R. Aaij *et al.* [LHCb Collaboration], *Phys. Rev. Lett.* **107**, 211801 (2011) [arXiv:1106.4435 [hep-ex]].
- [50] R. Aaij *et al.* [LHCb Collaboration], *Phys. Rev. D* **85**, 032008 (2012) [arXiv:1111.2357 [hep-ex]].
- [51] J. A. Bailey, A. Bazavov, C. Bernard, C. M. Bouchard, C. DeTar, D. Du, A. X. El-Khadra and J. Foley *et al.*, *Phys. Rev. D* **85**, 114502 (2012) [arXiv:1202.6346 [hep-lat]].
- [52] R. Aaij *et al.* [LHCb Collaboration], arXiv:1301.5286 [hep-ex].
- [53] L. Wolfenstein, *Phys. Rev. Lett.* **51**, 1945 (1983).
- [54] J. Charles, O. Deschamps, S. Descotes-Genon, R. Itoh, H. Lacker, A. Menzel, S. Monteil and V. Niess *et al.*, *Phys. Rev. D* **84**, 033005 (2011) [arXiv:1106.4041 [hep-ph]].
- [55] <http://www.utfit.org/UTfit/>
- [56] R. Fleischer, *Phys. Rept.* **370**, 537 (2002) [hep-ph/0207108].
- [57] P. Ball and R. Fleischer, *Eur. Phys. J. C* **48**, 413 (2006) [arXiv:hep-ph/0604249].
- [58] Z. Ligeti, M. Papucci and G. Perez, *Phys. Rev. Lett.* **97**, 101801 (2006) [hep-ph/0604112].
- [59] J. L. Rosner and M. Gronau, PoS BEAUTY **2011**, 045 (2011) [arXiv:1105.1923 [hep-ph]].

- [60] A. J. Buras, PoS BEAUTY **2011**, 008 (2011) [arXiv:1106.0998 [hep-ph]].
- [61] A. Lenz and U. Nierste, JHEP **0706**, 072 (2007) [arXiv:hep-ph/0612167]; arXiv:1102.4274 [hep-ph].
- [62] M. Ciuchini, E. Franco, V. Lubicz, F. Mescia and C. Tarantino, JHEP **0308**, 031 (2003) [arXiv:hep-ph/0308029].
- [63] A. Lenz, arXiv:1205.1444 [hep-ph].
- [64] H. Albrecht *et al.* [ARGUS Collaboration], *Phys. Lett. B* **192**, 245 (1987).
- [65] V. M. Abazov *et al.* [D0 Collaboration], *Phys. Rev. Lett.* **97**, 021802 (2006).
- [66] A. Abulencia *et al.* [CDF Collaboration], *Phys. Rev. Lett.* **97**, 062003 (2006).
- [67] R. Aaij *et al.* [LHCb Collaboration], *Phys. Lett. B* **709**, 177 (2012).
- [68] J. Beringer *et al.* [Particle Data Group], *Phys. Rev. D* **86**, 010001 (2012).
- [69] J. Laiho, E. Lunghi, and R.S. Van de Water, *Phys. Rev. D* **81**, 034503 (2010); the latest results are given at <http://www.latticeaverages.org>.
- [70] R. Aaij *et al.* [LHCb Collaboration], LHCb-CONF-2012-002.
- [71] I. Dunietz, R. Fleischer and U. Nierste, *Phys. Rev. D* **63**, 114015 (2001) [hep-ph/0012219].
- [72] R. Aaij *et al.* [LHCb Collaboration], *Phys. Lett. B* **709**, 2 (2012) [arXiv:1111.4183 [hep-ex]].
- [73] S. Descotes-Genon, J. Matias and J. Virto, *Phys. Rev. D* **85**, 034010 (2012) [arXiv:1111.4882 [hep-ph]].
- [74] R. Fleischer and R. Knegjens, *Eur. Phys. J. C* **71**, 1789 (2011) [arXiv:1109.5115 [hep-ph]].
- [75] R. Knegjens, arXiv:1209.3206 [hep-ph].
- [76] R. Aaij *et al.* [LHCb Collaboration] and A. Bharucha *et al.*, arXiv:1208.3355 [hep-ex].
- [77] Y. Grossman, *Phys. Lett. B* **380**, 99 (1996) [hep-ph/9603244].
- [78] L. Randall and S. Su, *Nucl. Phys. B* **540**, 37 (1999).
- [79] J.L. Hewett, arXiv:hep-ph/9803370 (1998).
- [80] G.W.S. Hou, arXiv:0810.3396 [hep-ph] (2008).
- [81] A. Soni *et al.*, *Phys. Lett. B* **683**, 302 (2010); A. Soni *et al.*, *Phys. Rev. D* **82**, 033009 (2010) and references therein.

- [82] M. Blanke *et al.*, J. High Energy Phys. **12**, 003 (2006); W. Altmannshofer, *et al.*, Nucl. Phys. B **830**, 17 (2010).
- [83] A. Buras and J. Girrbach, *Acta Phys. Polon. B* **43**, 1427 (2012) [arXiv:1204.5064 [hep-ph]].
- [84] [http://www.slac.stanford.edu/xorg/hfag/osc/fall\\_2012/HFAG\\_Chapter3\\_oct2012.pdf](http://www.slac.stanford.edu/xorg/hfag/osc/fall_2012/HFAG_Chapter3_oct2012.pdf) and references therein.
- [85] J. L. Rosner, *Phys. Rev. D* **42**, 3732 (1990).
- [86] A. S. Dighe, I. Dunietz, H. J. Lipkin and J. L. Rosner, *Phys. Lett. B* **369**, 144 (1996) [hep-ph/9511363].
- [87] A. S. Dighe, I. Dunietz and R. Fleischer, *Eur. Phys. J. C* **6**, 647 (1999) [hep-ph/9804253].
- [88] Y. Amhis *et al.* [Heavy Flavor Averaging Group Collaboration], arXiv:1207.1158 [hep-ex]; for online updates, see <http://www.slac.stanford.edu/xorg/hfag/>
- [89] Y. Xie, P. Clarke, G. Cowan and F. Muheim, *JHEP* **09**, 074 (2009).
- [90] R. Aaij *et al.* [LHCb Collaboration], *Phys. Rev. Lett.* **108**, 241801 (2012).
- [91] T. Aaltonen *et al.* [CDF Collaboration], *Phys. Rev. D* **83**, 052012 (2011) [arXiv:1102.1961 [hep-ex]].
- [92] R. Aaij *et al.* [LHCb Collaboration], *Phys. Rev. D* **86**, 071102 (2012) [arXiv:1208.0738 [hep-ex]].
- [93] R. Fleischer, arXiv:1212.2792 [hep-ph].
- [94] R. Aaij *et al.* [LHCb Collaboration], *Phys. Lett. B* **698**, 115 (2011) [arXiv:1102.0206 [hep-ex]].
- [95] J. Li *et al.* [Belle Collaboration], *Phys. Rev. Lett.* **106**, 121802 (2011) [arXiv:1102.2759 [hep-ex]].
- [96] T. Aaltonen *et al.* [CDF Collaboration], *Phys. Rev. D* **84**, 052012 (2011) [arXiv:1106.3682 [hep-ex]].
- [97] V. M. Abazov *et al.* [D0 Collaboration], *Phys. Rev. D* **85**, 011103 (2012) [arXiv:1110.4272 [hep-ex]].
- [98] S. Stone and L. Zhang, *Phys. Rev. D* **79**, 074024 (2009) [arXiv:0812.2832 [hep-ph]]; arXiv:0909.5442 [hep-ex].
- [99] P. Colangelo, F. De Fazio and W. Wang, *Phys. Rev. D* **83**, 094027 (2011) [arXiv:1009.4612 [hep-ph]].

- [100] R. Aaij *et al.* [LHCb Collaboration], *Phys. Lett. B* **713**, 172 (2012) [arXiv:1205.0934 [hep-ex]].
- [101] R. Fleischer, *Phys. Lett. B* **459**, 306 (1999) [hep-ph/9903456].
- [102] R. Fleischer, *Eur. Phys. J. C* **52**, 267 (2007) [arXiv:0705.1121 [hep-ph]].
- [103] R. Fleischer and R. Knegjens, *Eur. Phys. J. C* **71**, 1532 (2011) [arXiv:1011.1096 [hep-ph]].
- [104] A. Abulencia *et al.* [CDF Collaboration], *Phys. Rev. Lett.* **97**, 211802 (2006);  
M. Morello [CDF Collaboration], *Nucl. Phys. Proc. Suppl.* **170**, 39 (2007) [arXiv:hep-ex/0612018].
- [105] R. Louvot [Belle Collaboration], PoS E **PS-HEP2009**, 170 (2009) [arXiv:0909.2160 [hep-ex]].
- [106] M. Ciuchini, E. Franco, S. Mishima and L. Silvestrini, *JHEP* **1210**, 029 (2012) [arXiv:1205.4948 [hep-ph]].
- [107] G. Duplancić and B. Melić, *Phys. Rev. D* **78**, 054015 (2008) [arXiv:0805.4170 [hep-ph]].
- [108] R. Aaij *et al.* [LHCb Collaboration], LHCb-CONF-2012-007
- [109] M. Gronau and J. L. Rosner, *Phys. Lett. B* **482**, 71 (2000) [hep-ph/0003119].
- [110] R. Fleischer and R. Knegjens, arXiv:1012.0839 [hep-ph].
- [111] B. Aubert *et al.* [BABAR Collaboration], *Phys. Rev. Lett.* **99**, 021603 (2007).
- [112] S.W. Lin *et al.* [Belle Collaboration], *Nature* **452**, 332 (2008).
- [113] T. Aaltonen *et al.* [CDF Collaboration], *Phys. Rev. Lett.* **106**, 181802 (2011).
- [114] A. Alavi-Harati *et al.* [KTeV Collaboration], *Phys. Rev. D* **67**, 012005 (2003) [Erratum-ibid. *D* **70**, 079904 (2004)] [hep-ex/0208007].
- [115] J. R. Batley *et al.* [NA48 Collaboration], *Phys. Lett. B* **544**, 97 (2002) [hep-ex/0208009].
- [116] T. Aaltonen *et al.* [CDF Collaboration], *Phys. Rev. Lett.* **106**, 181802 (2011).
- [117] R. Aaij *et al.* [LHCb Collaboration], *Phys. Rev. Lett.* **108**, 201601 (2012) .
- [118] T. Aaltonen *et al.* [CDF Collaboration], Conference note 10726, <http://www-cdf.fnal.gov/physics/new/bottom/120628.blessed-Bhh9fb/>
- [119] R. Aleksan, I. Dunietz and B. Kayser, *Z. Phys. C* **54**, 653 (1992).
- [120] R. Fleischer, *Nucl. Phys. B* **671**, 459 (2003) [hep-ph/0304027].

- [121] G. Cavoto, R. Fleischer, T. Gershon, A. Soni, K. Abe, J. Albert, D. Asner and D. Atwood *et al.*, hep-ph/0603019.
- [122] V. Gligorov and G. Wilkinson, CERN-LHCB-2008-035.
- [123] V. Gligorov [LHCb Collaboration], arXiv:1101.1201 [hep-ex].
- [124] K. De Bruyn, R. Fleischer, R. Knegjens, M. Merk, M. Schiller and N. Tuning, *Nucl. Phys. B* **868**, 351 (2013) [arXiv:1208.6463 [hep-ph]].
- [125] T. Aaltonen *et al.* [CDF Collaboration], *Phys. Rev. Lett.* **103**, 191802 (2009). [arXiv:0809.0080 [hep-ex]].
- [126] R. Louvot *et al.* [Belle Collaboration], *Phys. Rev. Lett.* **102**, 021801 (2009) [arXiv:0809.2526 [hep-ex]].
- [127] R. Aaij *et al.* [LHCb Collaboration], *JHEP* **1206**, 115 (2012) [arXiv:1204.1237 [hep-ex]].
- [128] S. Nandi and U. Nierste, *Phys. Rev. D* **77**, 054010 (2008) [arXiv:0801.0143 [hep-ph]].
- [129] R. Aaij *et al.* [LHCb Collaboration], LHCb-CONF-2012-029, <http://cds.cern.ch/record/1477943/files/LHCb-CONF-2012-029.pdf>
- [130] R. Fleischer, *Eur. Phys. J. C* **51**, 849 (2007) [arXiv:0705.4421 [hep-ph]].
- [131] R. Aaij *et al.* [LHCb Collaboration], arXiv:1302.5854 [hep-ex].
- [132] R. Fleischer, *Phys. Rev. D* **60**, 073008 (1999) [hep-ph/9903540].
- [133] S. Descotes-Genon, J. Matias and J. Virto, *Phys. Rev. D* **76**, 074005 (2007) [Erratum-ibid. *D* **84**, 039901 (2011)] [arXiv:0705.0477 [hep-ph]].
- [134] R. Fleischer and M. Gronau, *Phys. Lett. B* **660**, 212 (2008) [arXiv:0709.4013 [hep-ph]].
- [135] B. Bhattacharya, A. Datta, M. Imbeault and D. London, *Phys. Lett. B* **717**, 403 (2012) [arXiv:1203.3435 [hep-ph]].
- [136] A. Datta, M. Duraisamy and D. London, *Phys. Rev. D* **86**, 076011 (2012) [arXiv:1207.4495 [hep-ph]].
- [137] T. Aaltonen *et al.* [CDF Collaboration], *Phys. Rev. Lett.* **107**, 261802 (2011) [arXiv:1107.4999. [hep-ph]].
- [138] R. Aaij *et al.* [LHCb Collaboration], *Phys. Lett. B* **713**, 369 (2012).
- [139] A. Datta, M. Duraisamy and D. London, *Phys. Lett. B* **701**, 357 (2011) [arXiv:1103.2442 [hep-ph]].

- [140] M. Gronau and J. L. Rosner, *Phys. Rev. D* **84**, 096013 (2011) [arXiv:1107.1232 [hep-ph]].
- [141] A. J. Buras, J. Girrbach, D. Guadagnoli and G. Isidori, *Eur. Phys. J. C* **72**, 2172 (2012) [arXiv:1208.0934 [hep-ph]].
- [142] G. Buchalla, A. J. Buras and M. E. Lautenbacher, *Rev. Mod. Phys.* **68**, 1125 (1996) [hep-ph/9512380].
- [143] W. Altmannshofer, P. Paradisi and D. M. Straub, *JHEP* **1204**, 008 (2012) [arXiv:1111.1257 [hep-ph]].
- [144] R. Aaij et al. [LHCb Collaboration], *Phys. Rev. Lett.* **108**, 231801 (2012) [arXiv:1203.4493].
- [145] A. J. Buras, F. De Fazio and J. Girrbach, *JHEP* **1302**, 116 (2013) [arXiv:1211.1896 [hep-ph]].
- [146] A. J. Buras, F. De Fazio, J. Girrbach and M. V. Carlucci, *JHEP* **1302**, 023 (2013) [arXiv:1211.1237 [hep-ph]].
- [147] A. J. Buras and J. Girrbach, *JHEP* **1301**, 007 (2013) [arXiv:1206.3878 [hep-ph]].
- [148] W. Altmannshofer, M. Carena, N. Shah and F. Yu, *JHEP* **1301**, 160 (2013) [arXiv:1211.1976 [hep-ph]].
- [149] K. Kowalska, S. Munir, L. Roszkowski, E. M. Sessolo, S. Trojanowski and Y.-L. S. Tsai, arXiv:1211.1693 [hep-ph].
- [150] U. Haisch and F. Mahmoudi, *JHEP* **1301**, 061 (2013) [arXiv:1210.7806 [hep-ph]].
- [151] O. Buchmueller, R. Cavanaugh, M. Citron, A. De Roeck, M. J. Dolan, J. R. Ellis, H. Flücher and S. Heinemeyer *et al.*, *Eur. Phys. J. C* **72**, 2243 (2012) [arXiv:1207.7315 [hep-ph]].
- [152] T. Hurth and F. Mahmoudi, *Nucl. Phys. B* **865**, 461 (2012) [arXiv:1207.0688 [hep-ph]].
- [153] W. Altmannshofer and D. M. Straub, *JHEP* **1208**, 121 (2012) [arXiv:1206.0273 [hep-ph]].
- [154] D. Becirevic, N. Kosnik, F. Mescia and E. Schneider, *Phys. Rev. D* **86**, 034034 (2012) [arXiv:1205.5811 [hep-ph]].
- [155] F. Mahmoudi, S. Neshatpour and J. Orloff, *JHEP* **1208**, 092 (2012) [arXiv:1205.1845 [hep-ph]].
- [156] T. Li, D. V. Nanopoulos, W. Wang, X.-C. Wang and Z. -H. Xiong, *JHEP* **1207**, 190 (2012) [arXiv:1204.5326 [hep-ph]].
- [157] A. Ali, B. D. Pecjak, and C. Greub, *Eur. Phys. J. C* **55**, 577 (2008).

- [158] J. Wicht *et al.* [Belle Collaboration] *Phys. Rev. Lett.* **100**, 121801 (2008).
- [159] R. Aaij *et al.* [LHCb Collaboration], *Phys. Rev. D* **85**, 112013 (2012).
- [160] F. Muheim, Y. Xie and R. Zwicky, *Phys. Lett. B* **664**, 174 (2008) [arXiv:0802.0876 [hep-ph]].
- [161] C. Bobeth, G. Hiller and G. Piranishvili, *JHEP* **0807**, 106 (2008) [arXiv:0805.2525 [hep-ph]].
- [162] CDF Collab. [http://www-cdf.fnal.gov/physics/new/bottom/120628.blessed-b2smumu\\_96/](http://www-cdf.fnal.gov/physics/new/bottom/120628.blessed-b2smumu_96/)
- [163] R. Aaij *et al.* [LHCb Collaboration], LHCb-CONF-2012-003